SPECIAL REPORT

INVESTIGATION OF ELECTRIFICATION OF POWDERS IN FLOW THROUGH TUBES AND NOZZLES. II. CHARGE ANALYSES OF DEAGGLOMERATED POWDERS

by

T. G Owe Berg and W. J. Flood

Contract DA-18-108-405-CML-829

Report 0395-04(14)SP November 1963

ORDNANCE DIVISION

Aerojet-General CORPORATION
A SUBSIDIARY OF THE GENERAL TIRE & RUBBER COMPANY
AZUSA, SACRAMENTO, AND DOWNEY, CALIFORNIA

AEROJET-GENERAL CORPORATION
Ordnance Research Division
11711 Woodruff Avenue
Downey, California

INVESTIGATION OF ELECTRIFICATION OF POWDERS IN FLOW THROUGH TUBES AND NOZZLES. II. CHARGE ANALYSES OF DEAGGLOMERATED POWDERS

by

T. G. Owe Berg and W. J. Flood

Investigations Under U. S. Army Chemical Center

Contract DA-18-108-405-CML-829

Report 0395-04(14)SP

Approved by: L. Zernow, Manager
Ordnance Research Division

Date: November 1963

No. of Pages: 68

Classification: UNCLASSIFIED

ABSTRACT

Charge measurements were conducted with airborne powders flowing out of a capillary tube at flow rates between 100 and 500 cc/min., corresponding to 3 and 15 m/s linear flow rate. The relative humidity of the air was 10%. The powders were saccharin, Carbowax 6000, Cab-O-Sil, and the two former materials with 1% of Cab-O-Sil as a deagglomerant. The MMD particle sizes were 7, 14, and 0.02 μ, respectively.

The dependence of the positive and negative charges per gram of material and of the abundances of positively and negatively charged material upon the flow rate were determined. The bearing of these quantities upon agglomeration is discussed with respect to flowing powders and aerosols. The effects of the deagglomerant are different in the two cases and depend upon the nature of the powder and upon the flow rate.

It is concluded that a deagglomerant may be effective as a free-flowing agent by causing large agglomerates, although smaller than those in the pure material, and by causing nearly equal abundances of positive and negative particles. Both effects are ruinous to presized aerosol material.

CONTENTS

		Page
1.	INTRODUCTION	1
2.	EXPERIMENTAL PROCEDURE	2
3.	EXPERIMENTAL RESULTS	4
4.	ANALYSIS OF EXPERIMENTAL DATA	13
	4.1 SACCHARIN	21
	4.2 SACCHARIN + 1% CAB-O-SIL	27
	4.3 CAB-O-SIL	30
	4.4 CARBOWAX 6000	39
	4.5 CARBOWAX 6000 + 1% CAB-O-SIL	40
5.	AGGLOMERATION IN POWDERS AND AEROSOLS	45
6.	DISCUSSION	49
7.	CONCLUSION	58

ILLUSTRATIONS

Figure		Page
1.	Aerosol Generator (dimensions in mm)	3
2.	Total positive charge deposited in 1 min Q_+ as function of flow rate v. ⊙ Saccharin, × Saccharin + 1% Cab-O-Sil	5
3.	Total positive charge deposited in 1 min Q_+ as function of flow rate square v^2. ▽ Carbowax 6000, ▲ Cab-O-Sil, + Carbowax 6000 + 1% Cab-O-Sil	6
4.	Total negative charge deposited in 1 min Q_- as a function of flow rate square v^2 ⊙ Saccharin, × Saccharin + 1% Cab-O-Sil	7
5.	Total negative charge deposited in 1 min Q_- as a function of flow rate v. ▽ Carbowax 6000, ▲ Cab-O-Sil, + Carbowax 6000 + 1% Cab-O-Sil	8
6.	Weight of positive deposit in 1 min W_+ as a function of flow rate v. ⊙ Saccharin, × Saccharin + 1% Cab-O-Sil	9
7.	Weight of positive deposit in 1 min W_+ as a function of flow rate v. ▽ Carbowax 6000, ▲ Cab-O-Sil, + Carbowax 6000 + 1% Cab-O-Sil	10
8.	Weight of negative deposit in 1 min W_- as a function of flow rate v. ⊙ Saccharin, × Saccharin + 1% Cab-O-Sil, ▽ Carbowax 6000, ▲ Cab-O-Sil, + Carbowax 6000 + 1% Cab-O-Sil	11

ILLUSTRATIONS (cont.)

Figure		Page
9.	Total weight of deposits in 1 min $W = W_+ + W_-$ as a function of flow rate v. ⊙ Saccharin, × Saccharin + 1% Cab-O-Sil, ▽ Carbowax 6000, △ Cab-O-Sil, + Carbowax 6000 + 1% Cab-O-Sil	12
10.	Average charge per gram of positive deposit q_+ as a function of flow rate v. ⊙ Saccharin, × Saccharin + 1% Cab-O-Sil, ▽ Carbowax 6000, △ Carbowax 6000 + 1% Cab-O-Sil	14
11.	Average charge per gram of positive deposit q_+ as a function of flow rate square v^2 for Cab-O-Sil	15
12.	Average charge per gram of negative deposit q_- as a function of flow rate v. ⊙ Saccharin, × Saccharin + 1% Cab-O-Sil, ▽ Carbowax 6000, △ Cab-O-Sil, + Carbowax 6000 + 1% Cab-O-Sil	16
13.	Total average absolute charge per gram $q = Q_+ + Q_-/W$ as a function of flow rate v. ⊙ Saccharin, × Saccharin + 1% Cab-O-Sil, △ Cab-O-Sil	17
14.	Total average absolute charge per gram $q = Q_+ + Q_-/W$ as a function of flow rate v. ▽ Carbowax 6000, + Carbowax 6000 + 1% Cab-O-Sil	18
15.	Ratio of weights of positive and negative deposits W_+/W_- as a function of flow rate v. ▽ Carbowax 6000, + Carbowax 6000 + 1% Cab-O-Sil	19

ILLUSTRATIONS (cont.)

Figure		Page
16.	Ratio of weights of negative and positive deposits W_-/W_+ as a function of flow rate v. ⊙ Saccharin, × Saccharin + 1% Cab-O-Sil, Cab-O-Sil	20
17.	The product $q_+ \times q_-$ as a function of flow rate square v^2. ⊙ Saccharin, × Saccharin + 1% Cab-O-Sil, ▽ Carbowax 6000, + Carbowax 6000 + 1% Cab-O-Sil	23
18.	$P = Q_+ \times Q_-/W^2$ as a function of flow rate square v^2. ⊙ Saccharin, × Saccharin + 1% Cab-O-Sil	25
19.	Weights of positive deposit in 1 min W_+, negative deposit W_-, and sum of positive and negative deposits $W = W_+ + W_-$ as functions of flow rate v for the first run of Saccharin + 1% Cab-O-Sil. ⊙ W_+, × W_-, + W.	31
20.	Ratio of weights of negative and positive deposits in 1 min W_-/W_+ as a function of flow rate v for the first run of Saccharin 1% Cab-O-Sil	32
21.	Total positive charge Q_+ and total negative charge Q_- deposited in 1 min as functions of flow rate v and square of flow rate v^2, respectively, for the first run of Saccharin + 1% Cab-O-Sil	33
22.	Average charge per gram of positive deposit q_+, negative deposit q_-, and absolute charge q as functions of flow rate v for the first run of Saccharin + 1% Cab-O-Sil ⊙ q_+, × q_-, + q.	34

ILLUSTRATIONS (cont.)

Figure		Page
23.	Logarithm of the product $q_+ \times q_-$ as a function of flow rate v for Cab-O-Sil.	36
24.	$P = Q_+ \times Q_-/W^2$ as a function of v^4/v-35 for Cab-O-Sil	37
25.	$P = Q_+ \times Q_-/W^2$ as a function of flow rate v. [illegible] Carbowax 6000, + Carbowax 6000 + 1% Cab-O-Sil	42
26.	Schematic representation of "degree of agglomeration" as a function of the ratios W_+/W_- and W_-/W_+ at different values of the product $q_+ q_-$	48

1. INTRODUCTION

When a powder flows through a tube, the tube wall acquires a coat of the powder, and the flowing powder rubs against this coat. As a result of the friction, the flowing powder becomes electrically charged. When a powder is milled or generally handled, there is also such friction and electrification. In all these cases, the charges affect the properties of the powder, particularly by promoting agglomeration. This is of considerable importance in the production of aerosols because agglomeration increases the particle size. Furthermore, the charges acquired in the spraying of an aerosol affect the stability of the aerosol and also the effectiveness of the aerosol, e.g., an insecticide. [1)]

These effects have been studied extensively in a current research program. They are of particular importance at low humidities because few materials in particulate form can be handled at all at high humidities, and because electrification in friction is greatest at low humidities. The effects of the relative humidity of the air upon electrification and adhesion between powder particles are the subjects of preceding reports[2-4)].

According to Nash et al[5)], the addition of a deagglomerant reduces the charge and the agglomeration. Thus, the addition of 1% Cab-O-Sil to saccharin reduced the charge on the powder as it flowed out of a hole in the bottom of the container and also reduced the shear strength of the compacted powder.

It appears, therefore, that a deagglomerant could have drastic effects upon the properties of an aerosol by suppressing the charge. In order to study this and other electrification phenomena, an investigation has been conducted, in which airborne particles with and without an added deagglomerant have been analysed with respect to charge and charge distribution as they emerge from a capillary tube. The technique used in this investigation was described in a previous report[6)]. The results are presented and discussed in the following sections.

In order to keep this investigation within the frame of the current program, agglomeration per se was not included as an object of study. It turns out, however, that information on agglomeration may be derived from the results. It is therefore in order to discuss the results with respect to their bearing upon agglomeration in preparation for future investigations that include the study of agglomeration. This will be done in Sections 5 and 6.

The results show that a deagglomerant may affect the charge and the charge distribution more or less, depending upon the nature of the powder, to which it is added, and upon the flow rate. The deagglomerant may have different effects on different powders, and on the same powder at different flow rates. Thus, to take an extreme case, the deagglomerant could conceivably suppress agglomeration at low flow rates as in ordinary handling but promote agglomeration in the sprayed aerosol. As a consequence, a deagglomerant should be evaluated with respect to its effects upon the properties of the aerosol as well as those of the powder.

2. EXPERIMENTAL PROCEDURE

The experimental technique and the equipment used are described in a preceding report[6].

The materials were given to us by Mr. Nash of General Mills, Inc. They were:

Saccharin, MMD 7μ, size distribution ref. [5], p. 2-6
Carbowax 6000, MMD 14μ, size distribution ref. [5], p. 2-7
Cab-O-Sil, MMD 0.02 , ref. [5], p. 4-54
Saccharin + 1% Cab-O-Sil
Carbowax + 1% Cab-O-Sil

The powder was aerosolized in the apparatus shown in Figure 1. The powder is held in a container, which is vibrated, and the powder is stirred up by a stream of air of about 10% relative humidity. The aerosol is sucked into the charge analyzer by a separate pump. The flow rates in the two systems are thus controlled independently. The flow rate of the stirring air was kept constant at approximately 2000 cc/min, corresponding to a linear velocity of 3 cm/s. The flow rate in the charge analyzer was varied between 100 and 500 cc/min, corresponding to a linear velocity of 3 to 15 m/s.

There was noticeable agglomeration of the powder in the aerosol generator, and the particle size was certainly larger than the nominal size. The size of the agglomerates was not assessed.

No effort was made to maintain a constant aerosol density. Previous experience[6] has shown that the charge per gram of material is independent of the density over a wide range. This holds also in this investigation.

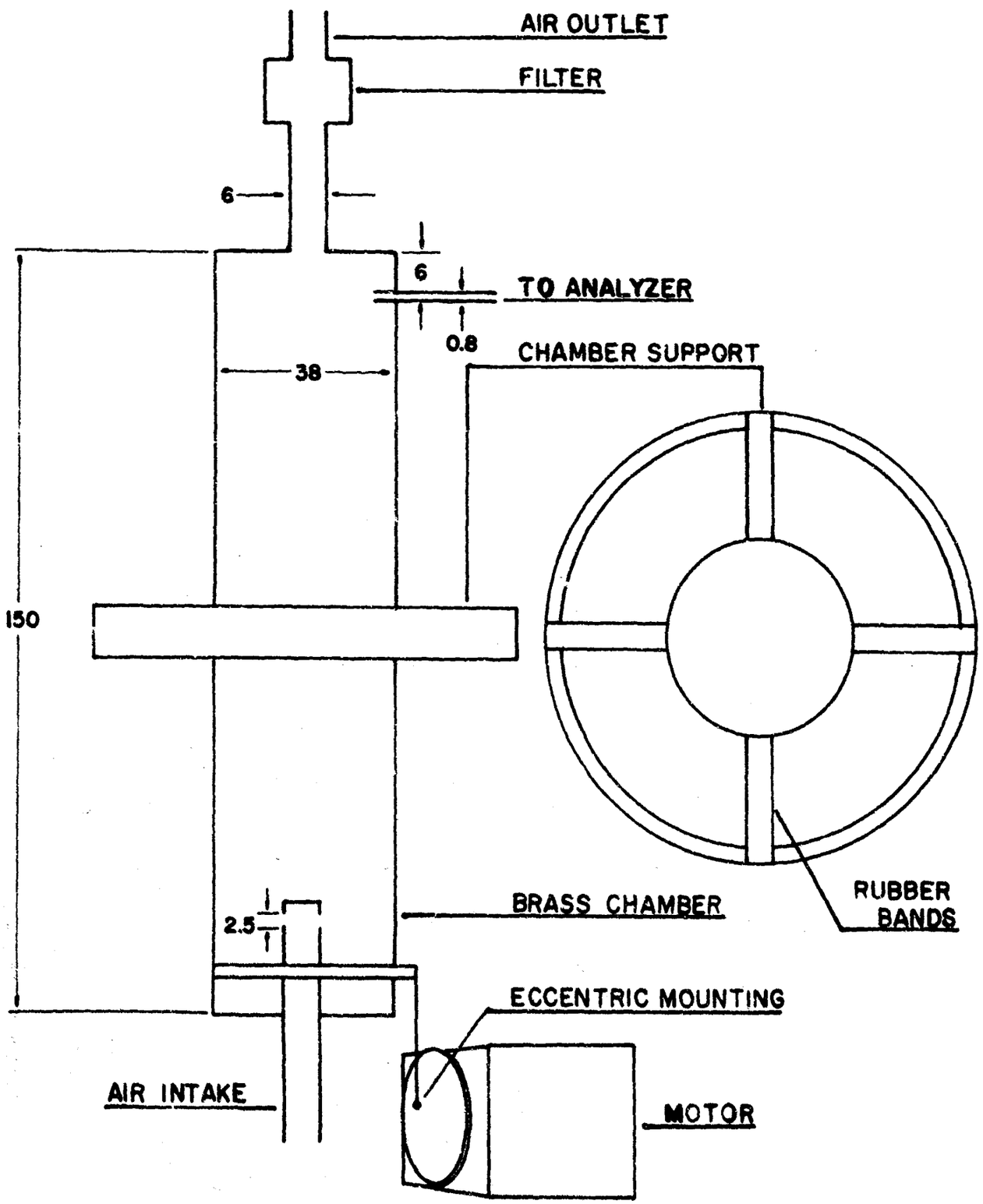

Figure 1. Aerosol Generator (Dimensions in mm).

It was pointed out in the preceding report[6] that the charge analyzer does not work well at high humidities of the air because the humidity reduces the insulation resistance. The most obnoxious result of this effect is a shift of the zero level of the charge record. This reduces the accuracy of the charge measurement much more than does the leakage current. In order to avoid this error, it is necessary to operate the charge analyzer at a low enough humidity. This is not considered to be a restriction to the usefulness of the charge analyzer because fine powders cannot be handled at high humidities anyway. It was found that a relative humidity of the air of 10% is adequate. This happens to be the relative humidity of the air from our compressor, and the use of air of this humidity was therefore adopted in these experiments.

In another investigation, following upon the one treated in this report, it appeared that further drying of the air caused the data to become erratic, and occasionally no charge at all was recorded. This may be a result of poor adherence of the aerosol material to the tube wall so that the tube wall is not coated by the aerosol material but left bare. This issue has not been studied as yet.

3. EXPERIMENTAL RESULTS

The primary measured quantities are total positive charge Q_+ total negative charge Q_-, weight of positive deposit W_+ and weight of negative deposit W_-, all in a period of 1 min. There was no neutral deposit in these experiments. These primary quantities are plotted against the flow rate in Figures 2 to 8.

At a constant density of material, expressed as weight of powder per unit volume of air, the total deposit,

$$W = W_+ + W_- \tag{1}$$

is proportional to the flow rate. This quantity is plotted against the flow rate in Figure 9.

Derived quantities of particular interest are the average positive and negative charges per gram,

$$q_+ = \frac{Q_+}{W_+} \tag{2}$$

$$q_- = \frac{Q_-}{W_-} \tag{3}$$

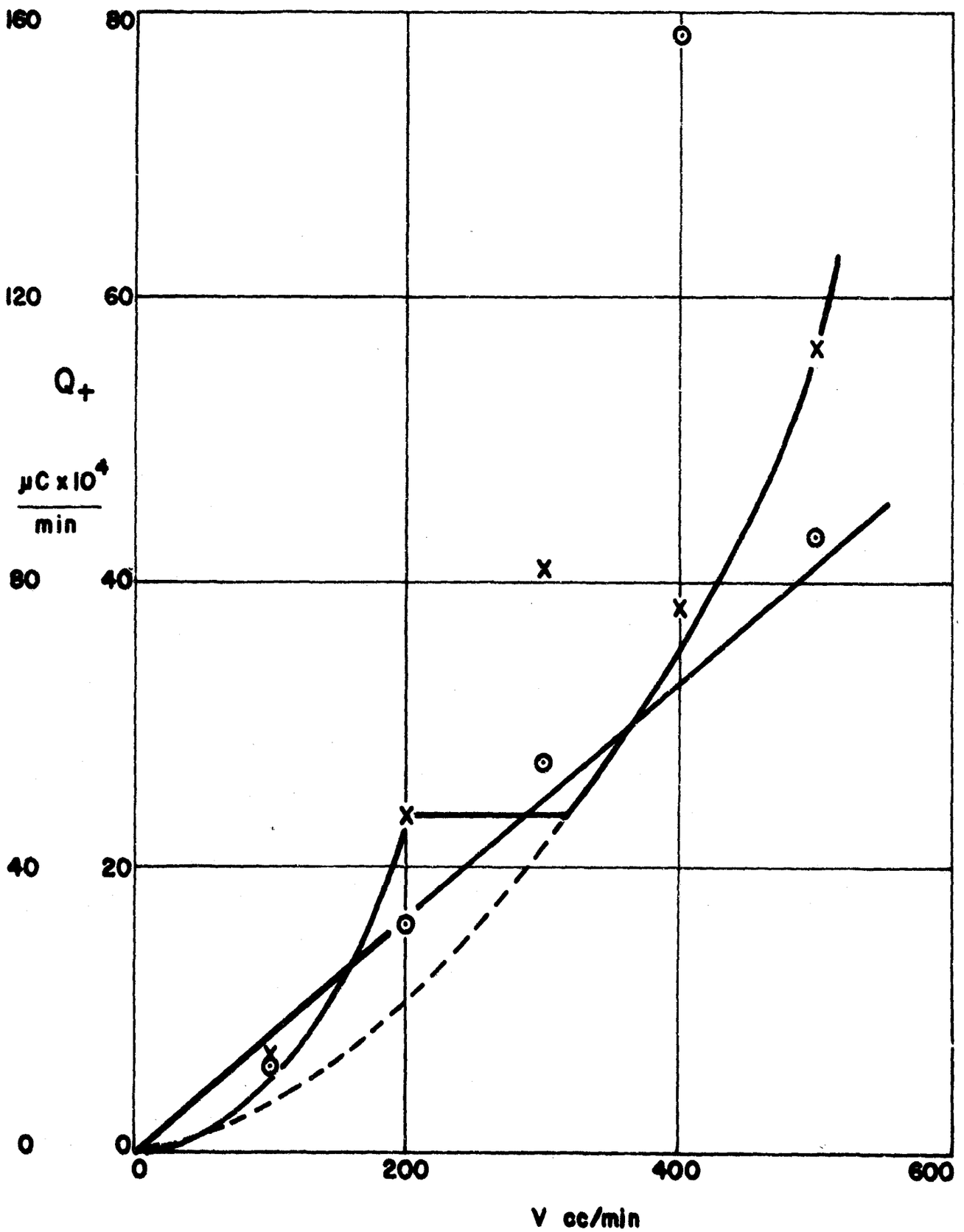

Figure 2. Total Positive Charge Deposited in 1 . . . Q_+ as Function of Flow Rate v.
○ Saccharin, × Saccharin + 1% Cab-O-Sil

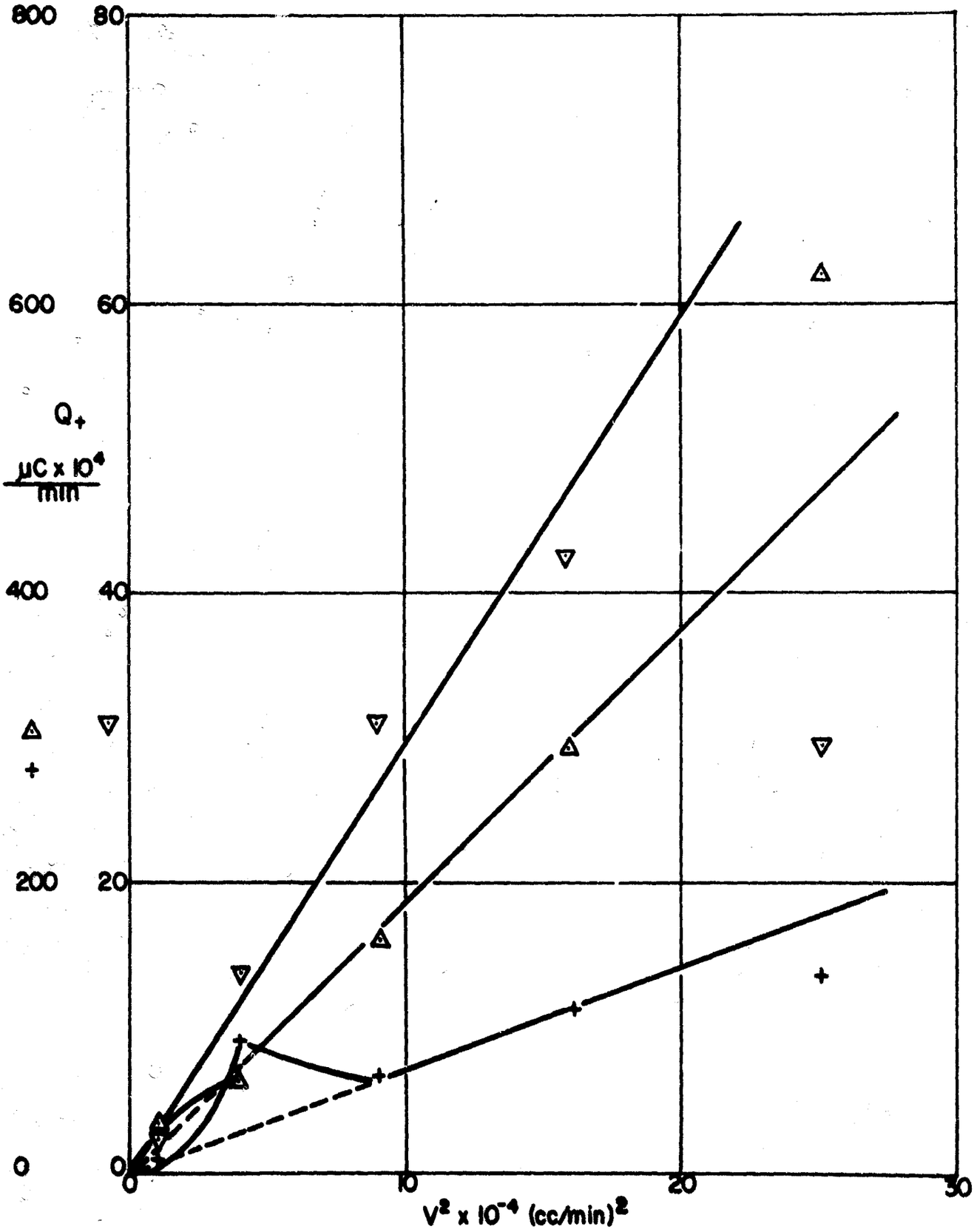

Figure 3. Total positive charge deposited in 1 min Q as function of low rate square v^2. ▽ Carbowax 6000, △ Cab-O-Sil, + Carbowax 6000 + 1% Cab-O-Sil.

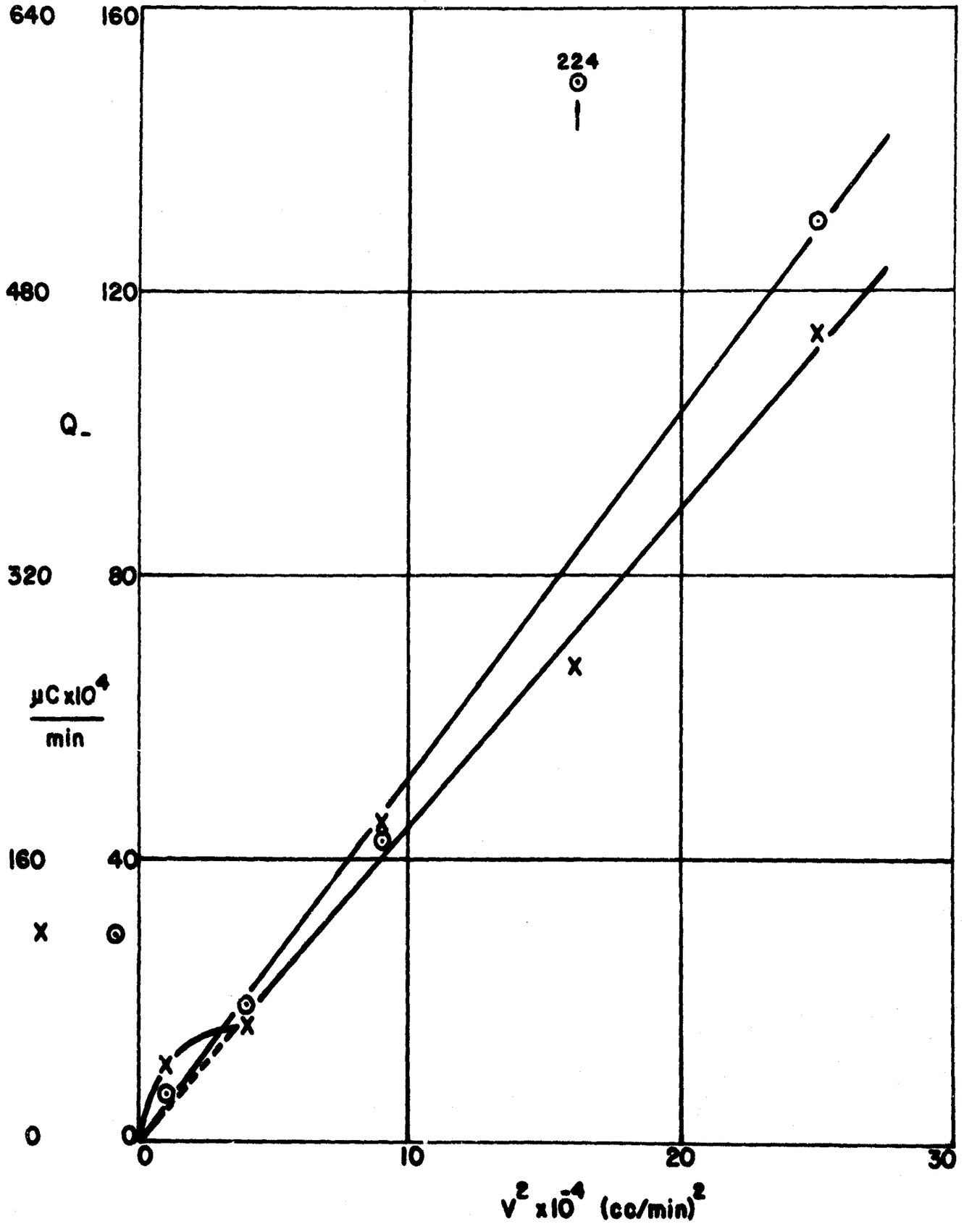

Figure 4. Total negative charge deposited in 1 min Q_- as a function of flow rate square v^2, ⊙ Saccharin, X Saccharin + 1% Cab-O-Sil.

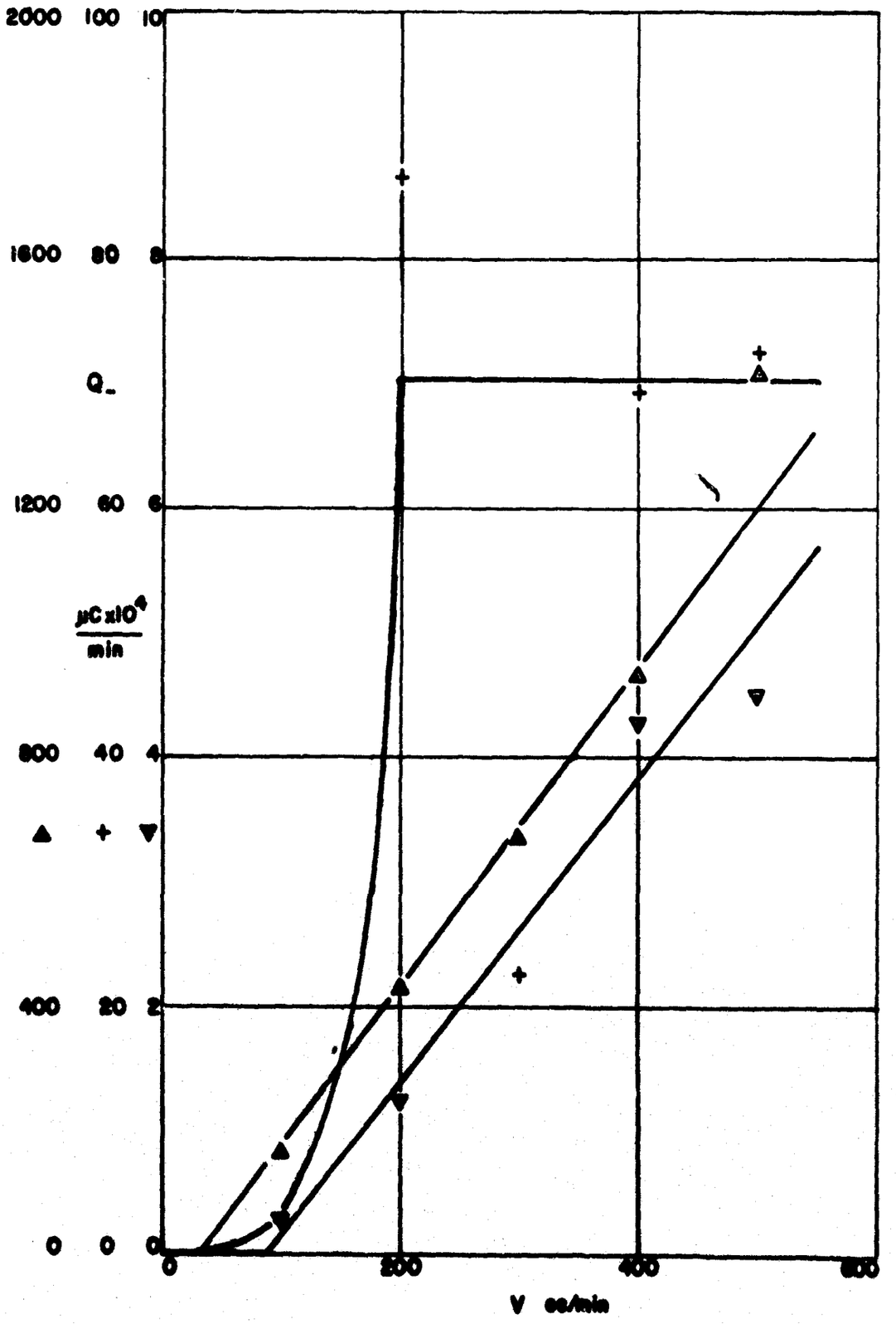

Figure 5. Total negative charge deposited in 1 min Q_- as a function of flow rate v. ▼ Carbowax 6000, ▲ Cab-O-Sil, + Carbowax 6000 + 1% Cab-O-Sil.

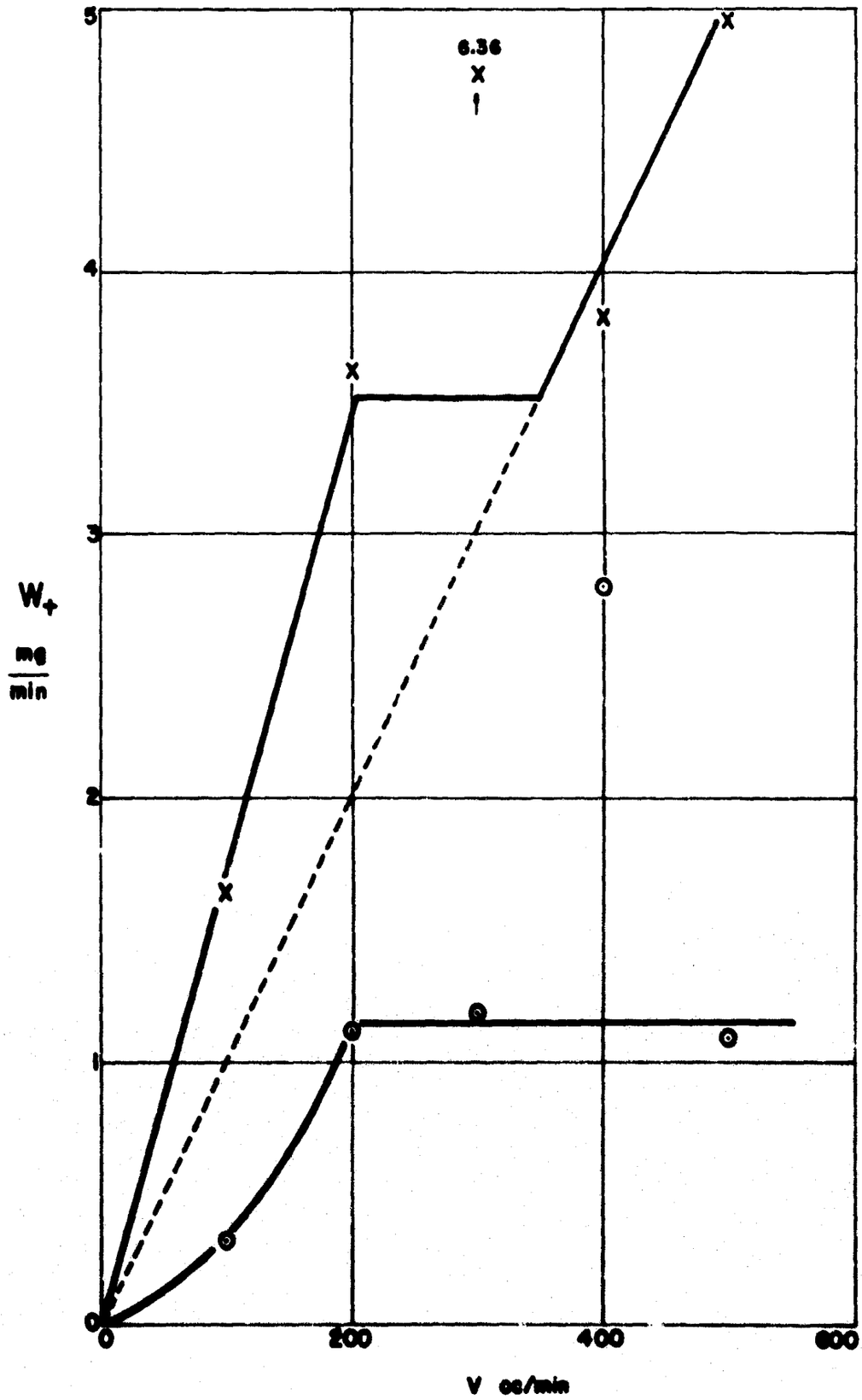

Figure 6. Weight of positive deposit in 1 min W_+ as a function of flow rate v. Saccharin, X Saccharin + 1% Cab-O-Sil.

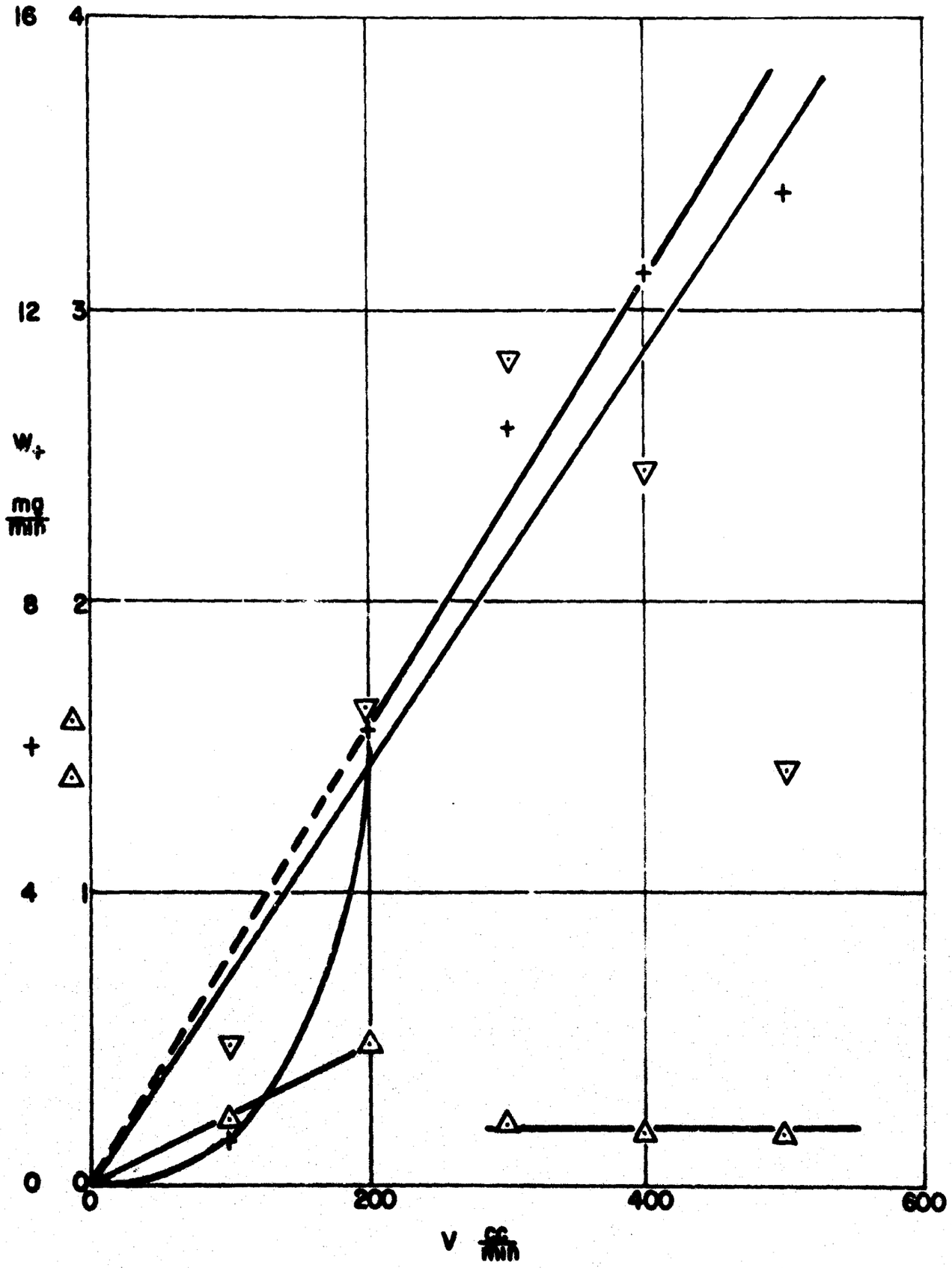

Figure 7. Weight of positive deposit in 1 min W_+ as a function of flow rate v. Carbowax 6000, Cab-O-Sil, + Carbowax 6000 + 1% Cab-O-Sil.

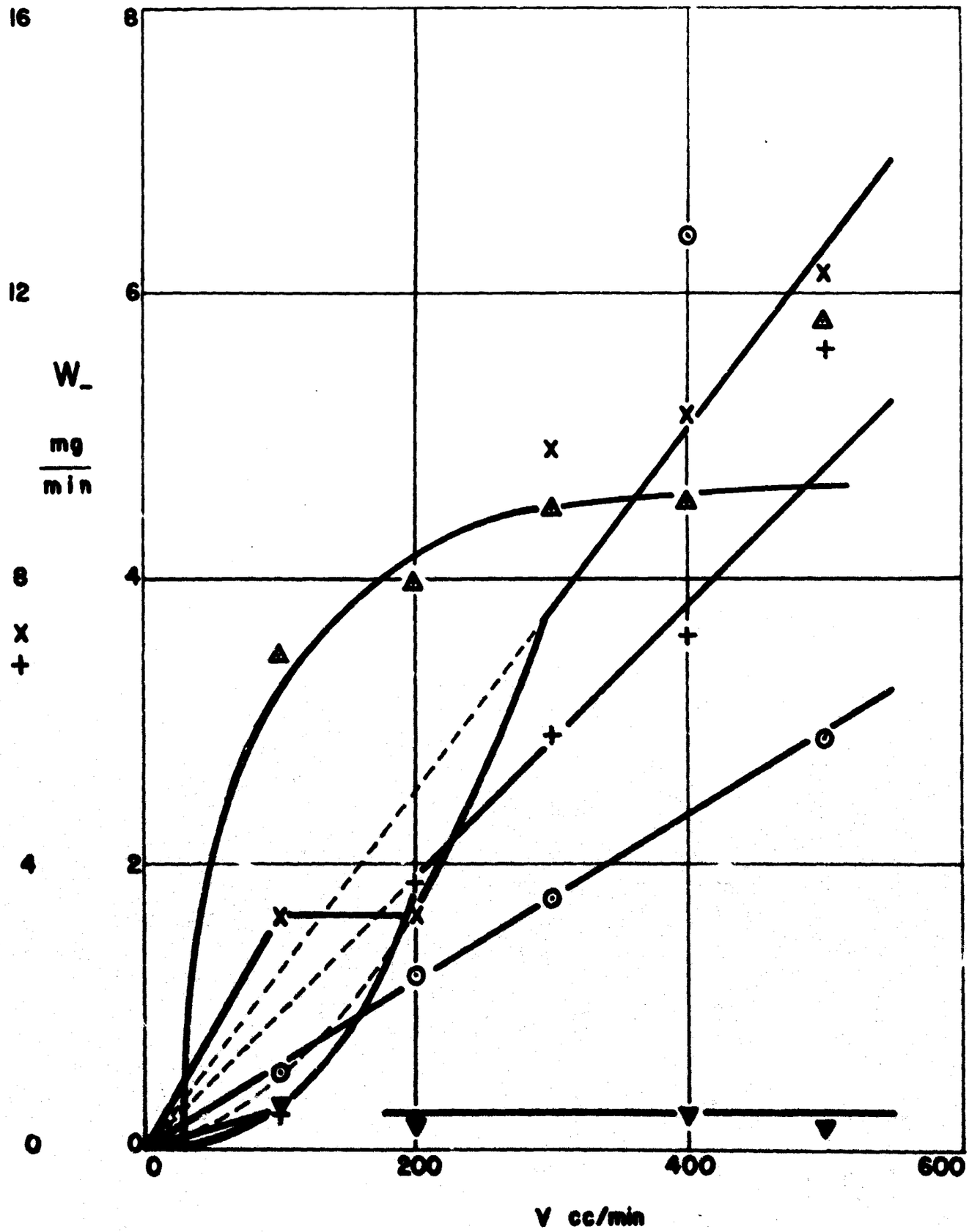

Figure 8. Weight of negative deposit in 1 min W_- as a function of flow rate v. Saccharin, X Saccharin + 1% Cab-O-Sil, Carbowax 6000, Δ Cab-O-Sil, + Carbowax 6000 + 1% Cab-O-Sil.

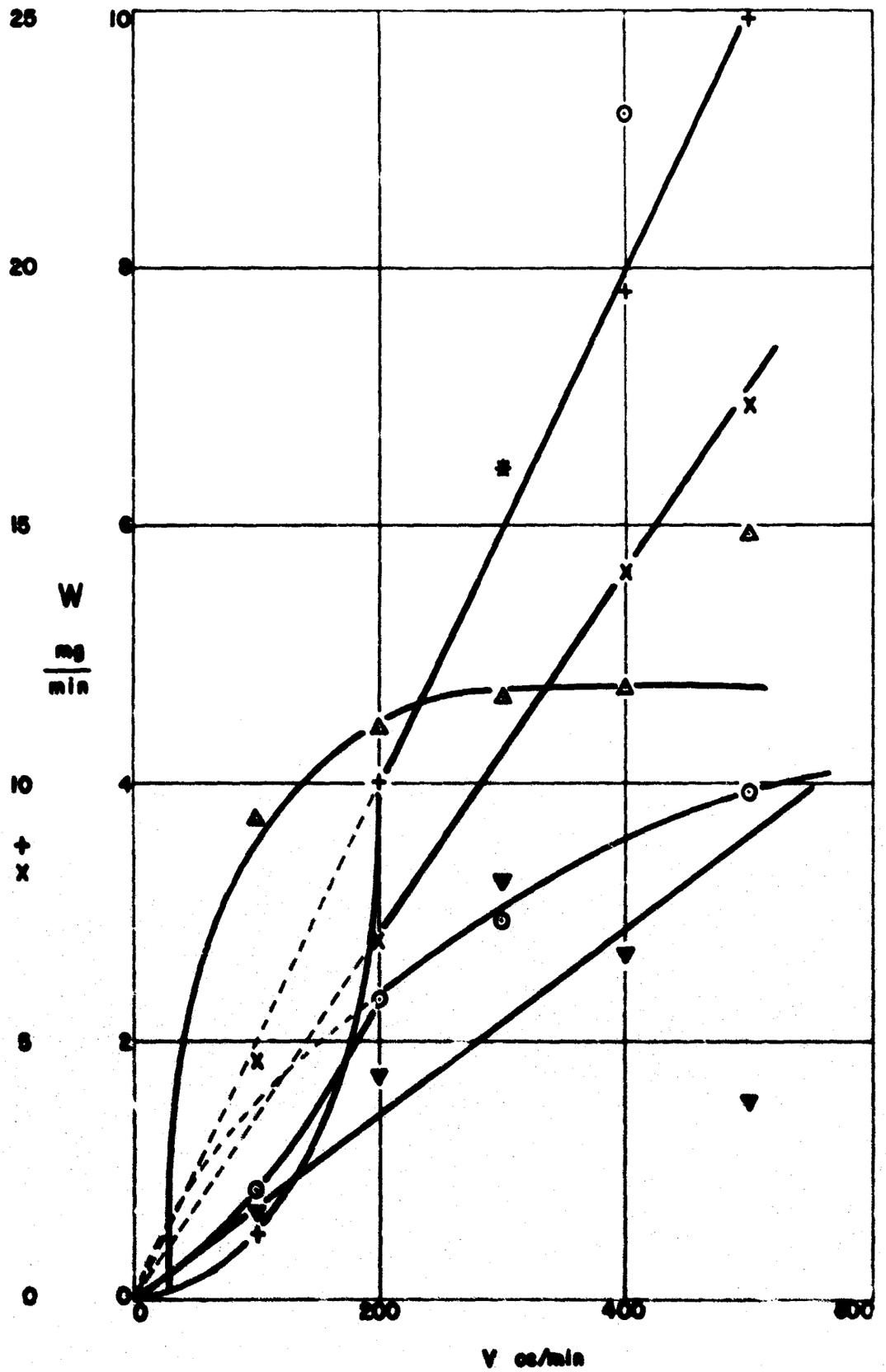

Figure 9. Total weight of deposits in 1 min. W = $W_+ + W_-$ as a function of flow rate v. Saccharin, × Saccharin + 1% Cab-O-Sil, Carbowax 6000, Cab-O-Sil, + Carbowax 6000 + 1% Cab-O-Sil.

the average absolute charge per gram

$$q = \frac{Q_+ + Q_-}{W} \tag{4}$$

and the ratio W_+/W_-. These quantities are plotted against the flow rate in Figures 10 to 16.

The scatter of the points in some of these plots is so great as to make it almost impossible to draw meaningful curves. This scatter is not a result of inaccuracy of the measurements but is a feature of the phenomena under study. Thus, the scatter in the values of q, q_+ and q_- is little as compared to that in the values of the primary quantities, and the scatter in the data for the materials of a single component is little as compared to that in the same data for the mixtures.

In the case of Carbowax 6000 + 1% Cab-O-Sil, the large Carbowax 6000 particles are coated with the small Cab-O-Sil particles[5]. This coating may be expected to be more or less complete, and one may therefore expect the data to scatter as much as the coverage varies. The data may then vary between low values and those for Carbowax 6000 or Cab-O-Sil alone.

Another reason for scatter is variation in the coat of the material on the tube wall. In order to eliminate such scatter, the powder was blown for some time through the tube before the data were taken.

At the side of these two factors, the variations in the humidity of the air are probably of lesser effect.

It follows from this discussion already that the data are meaningful in spite of the scatter, and that the scatter as such is informative of the phenomenon. This point will be further discussed in Sections 4 and 6. The curves drawn on the data are based upon the analysis of the data presented in Section 4.

4. ANALYSIS OF EXPERIMENTAL DATA

A casual glance at some of the data gives an impression of a wild scatter that does not permit an analytical representation. On the other hand, some of the data fall on a straight line with remarkable precision. An instance of the wild scatter are the Q_- data

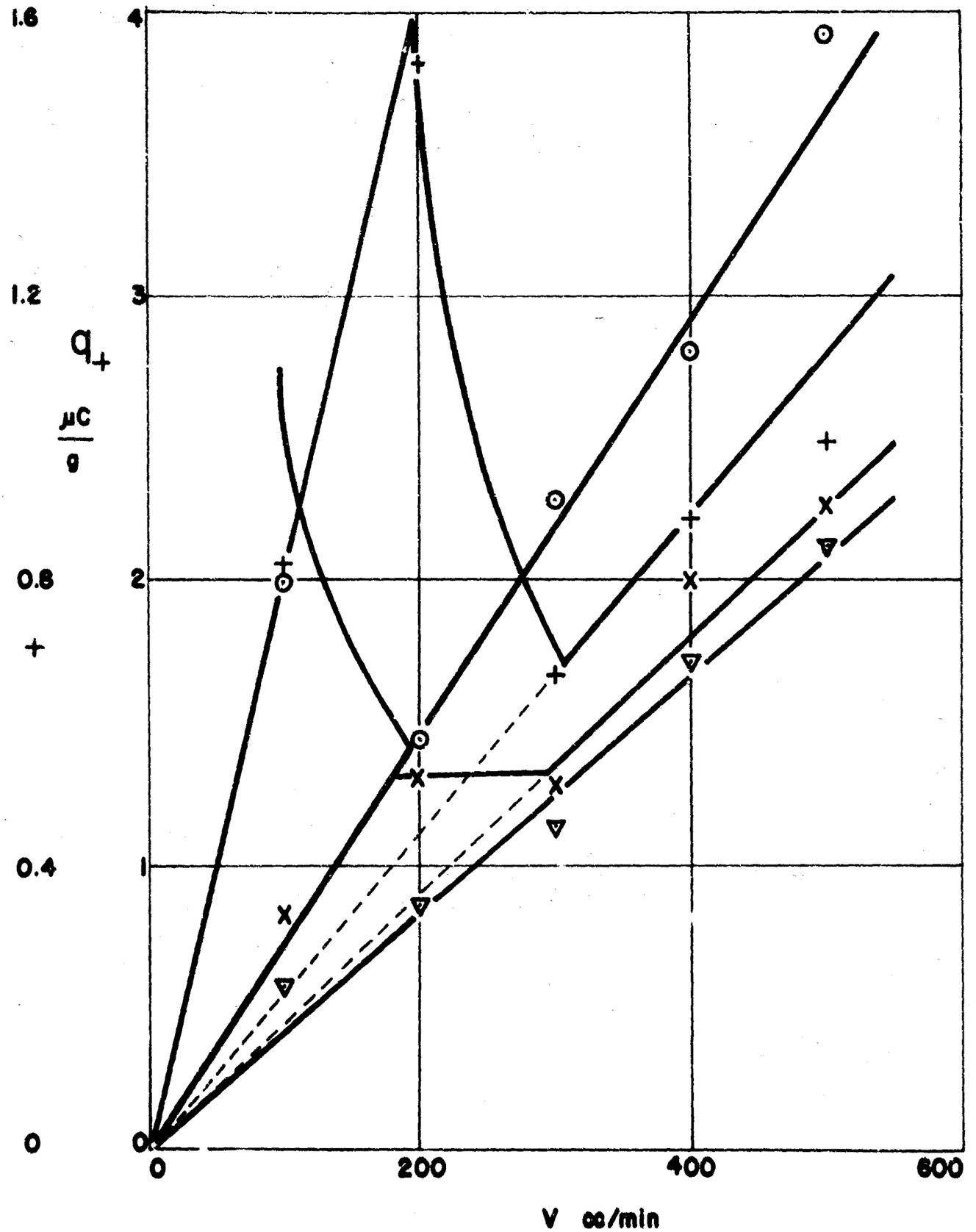

Figure 10. Average charge per gram of positive deposit q_+ as a function of flow rate v. ⊙ Saccharin, × Saccharin + 1% Cab-O-Sil, + Carbowax 6000, ▽ Carbowax 6000 + 1% Cab-O Sil.

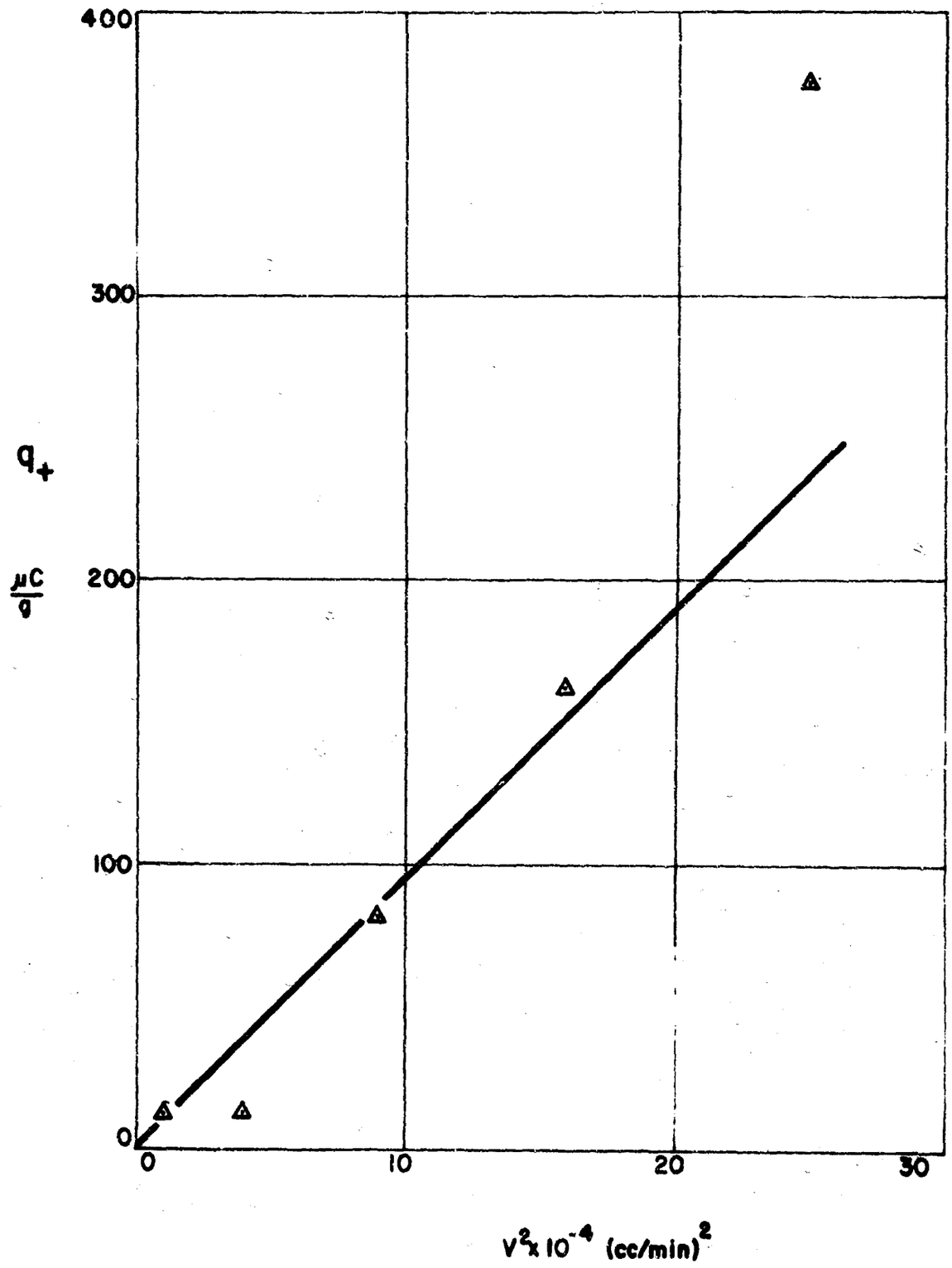

Figure 11. Average charge per gram of positive deposit q_+ function of flow rate square v^2 for Cab-O-Sil.

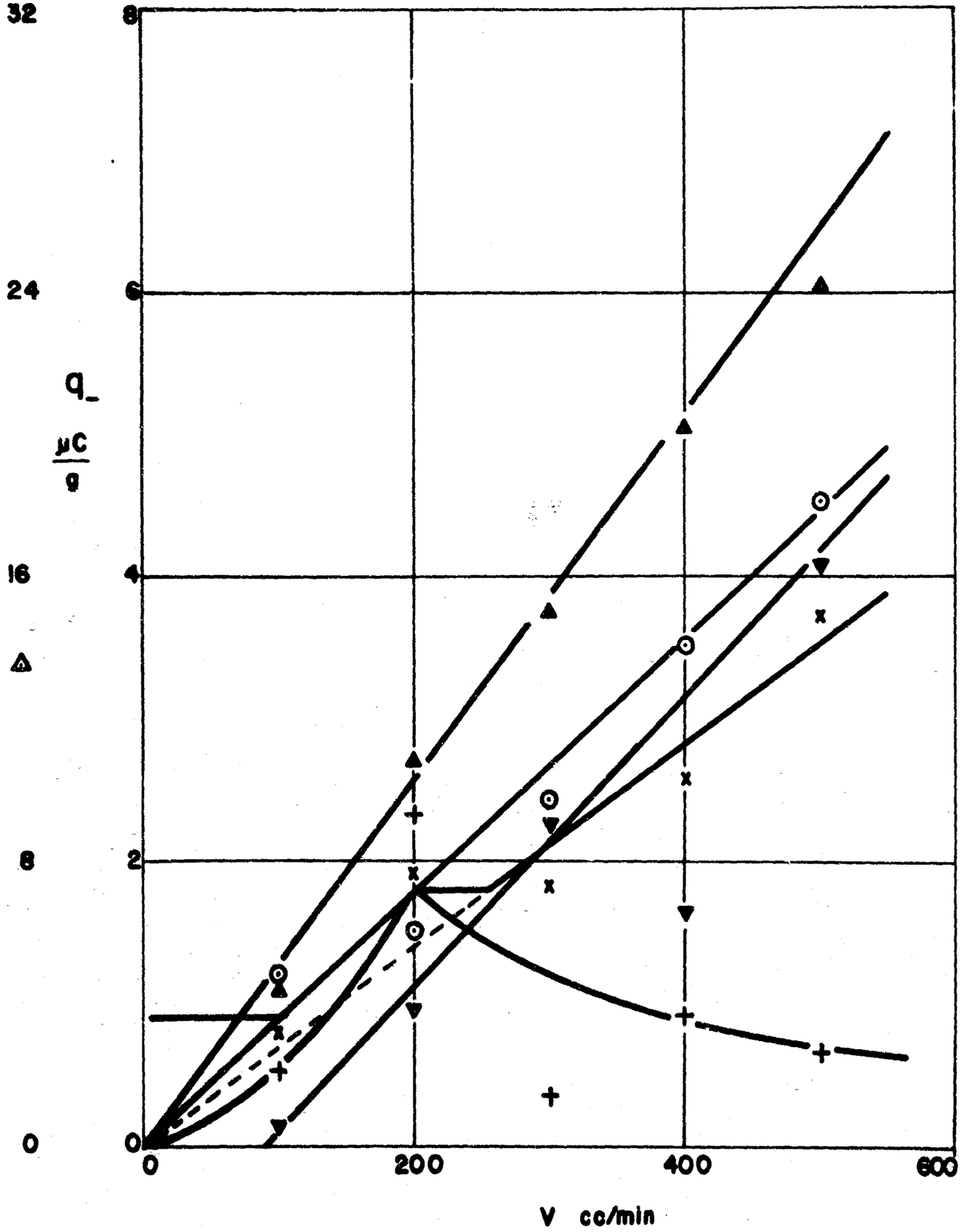

Figure 12. Average charge per gram of negative deposit q_ as a function of flow rate v. ⊙ Saccharin, X Saccharin + 1% Cab-O-Sil, ▼ Carbowax 6000, ▲ Cab-O-Sil, + Carbowax 6000 + 1% Cab-O-Sil.

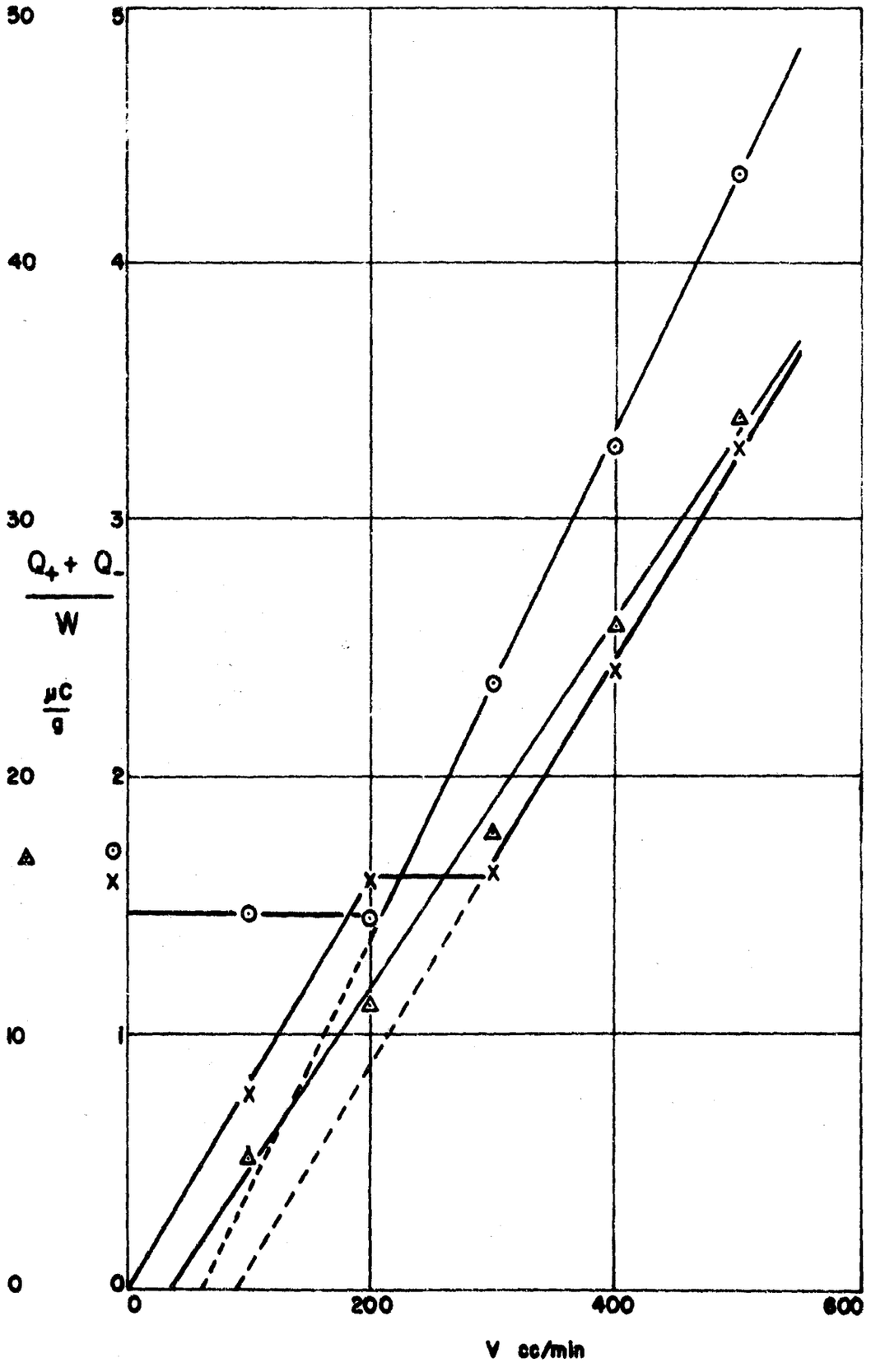

Figure 13. Total average absolute charge per gram $q = Q_+ + Q_- / W$ as a function of flow rate v. ⊙ Saccharin, X Saccharin + 1% Cab-O-Sil, △ Cab-O-Sil.

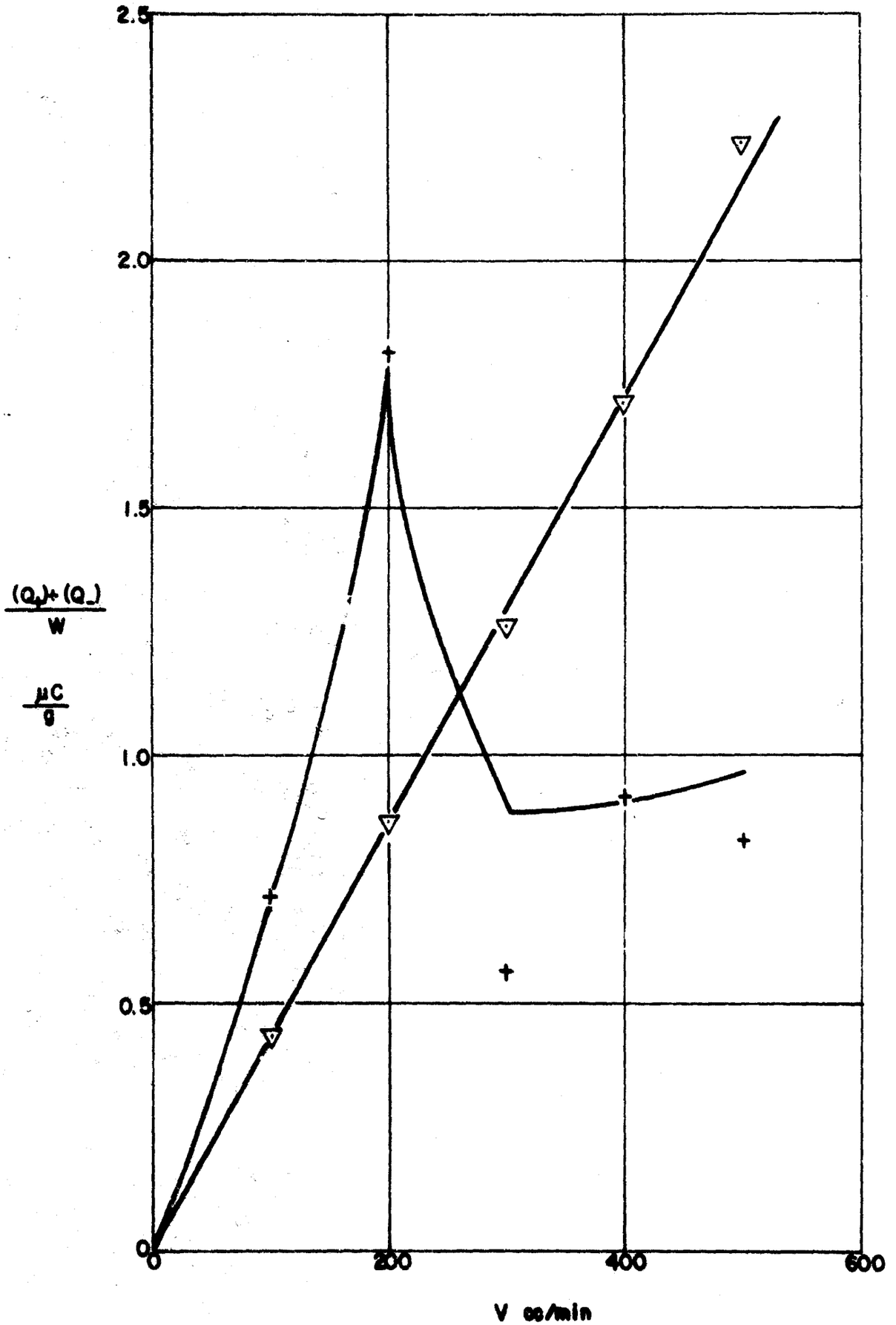

Figure 1 . Total average absolute charge per gram $q = (Q_+ + Q_-)/W$ as a function of flow rate v. Carbowax 6000, + Carbowax 6000 + 1% Cab-O-Sil.

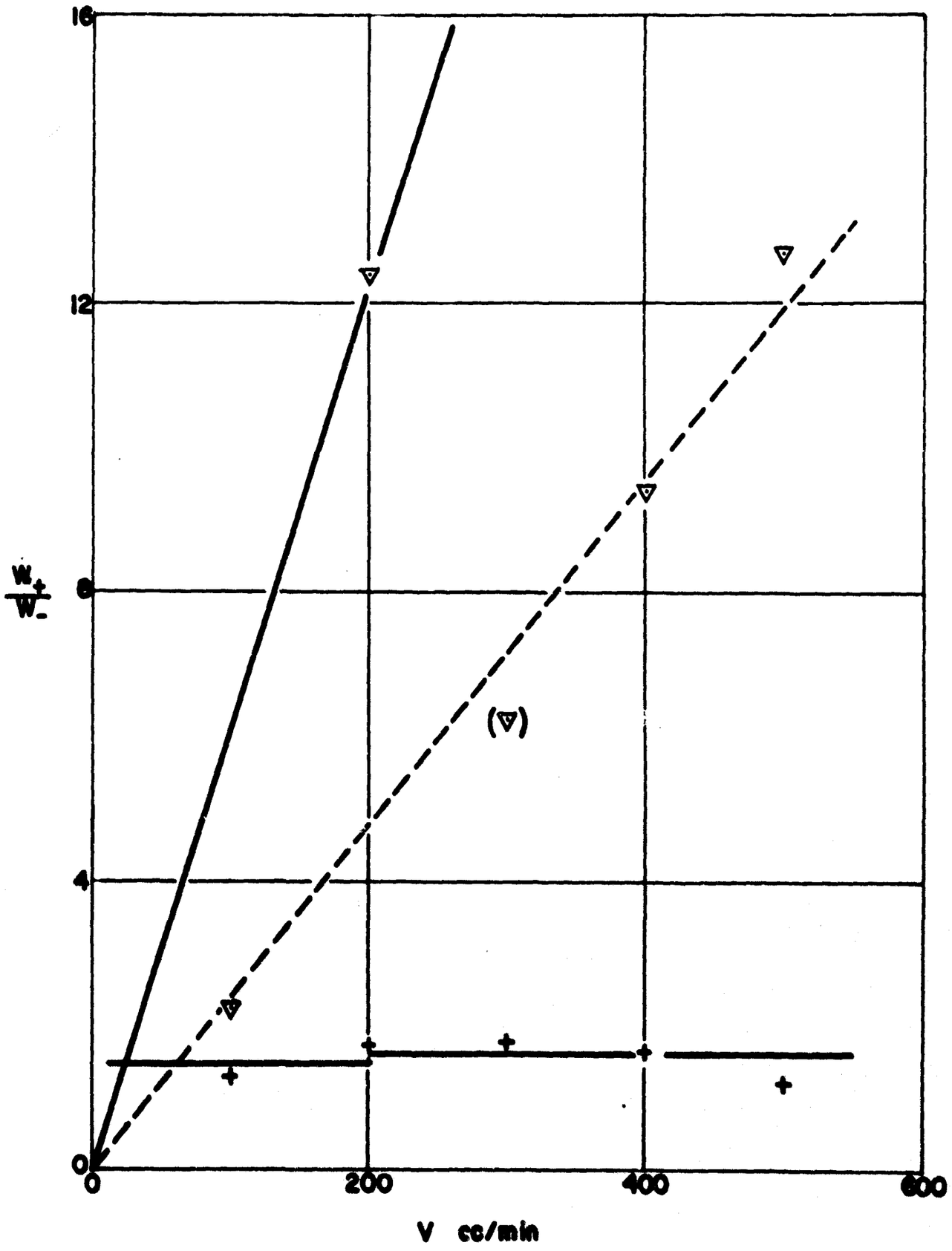

Figure 15. Ratio of weights of positive and negative deposits W_+ / W_- as a function of flow rate v ▽ Carbowax 6000, + Carbowax 6000 + 1% Cab-O-Sil.

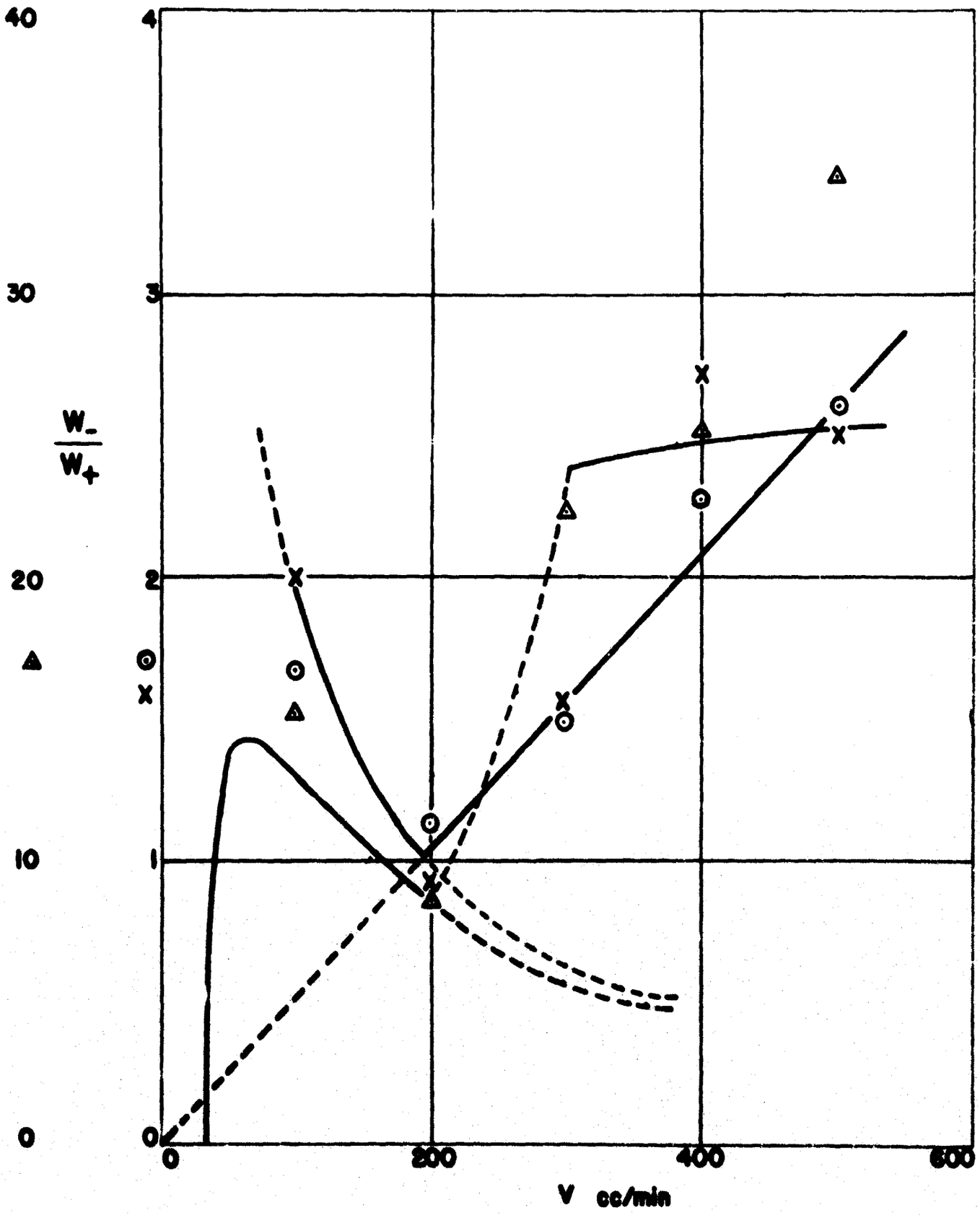

Figure 16. Ratio of weights of negative and positive deposits W_-/W_+ as a function of flow rate v. ⊙ Saccharin, X Saccharin + 1% Cab-O-Sil, △ Cab-O-Sil.

for Carbowax 6000 + 1% Cab-O-Sil in Figure 5. An instance of the high precision are the q data for Carbowax 6000 in Figure 14. It is clear that the accuracy of the measurements is very high and that the scatter is a feature of the phenomenon under study.

As already pointed out, the density of the airborne powder was not controlled, and there is no way to control it. This point will be discussed further in Section 6. Nevertheless, the plot in Figure 9 of W against v for Carbowax 6000 + 1% Cab-O-Sil is a remarkably good straight line, the slope of which is the density. Hence, there is nothing wrong with the aerosol generator. The corresponding plot for saccharin + 1% Cab-O-Sil is also fairly good. But the plots for the pure powders saccharin, Carbowax 6000, and Cab-O-Sil are far from linear. Since the deagglomerated powders have a constant density and the pure powders do not, the variations in the density must be a result of agglomeration. Accordingly, the deviation from proportionality between W and v give information on agglomeration in the powder.

The analysis of the data in this section is a purely mathematical operation. It is based upon the interrelation of the quantities under study, which makes it possible to calculate one from the others, and upon the observation referred to that the error of measurement is negligible. The interrelation between the quantities has the effect of increasing the number of observations. Actually, there are 5 values of v plus the origin, since Q_+, Q_-, W_+, W_-, and W must necessarily be zero at $v = 0$. This makes effectively 6 values of v. The interrelation between quantities effectively multiplies this number of observations.

4.1 SACCHARIN

The data for the positive deposits are fairly good. Q_+ and q_+ are proportional to v, and W_+ is constant at high flow rates. These data are thus consistent. The best fit of the data gives

Figure 6. $$W_+ = 1.140 \frac{mg}{min}, \quad v \geq 200 \frac{cc}{min} \tag{5}$$

Figure 10. $$q_+ = 7.22 v \times 10^{-3} \frac{\mu C}{g}, \quad v \geq 200 \frac{cc}{min} \tag{6}$$

Figure 2. $$Q_+ = 823 v \times 10^{-8} \frac{\mu C}{min}. \tag{7}$$

For the negative deposit we find

$$\text{Figure 8.} \quad W_- = 5.84\, v \times 10^{-3} \frac{mg}{min}, \tag{8}$$

$$\text{Figure 12.} \quad q_- = 8.91\, v \times 10^{-3} \frac{\mu C}{g} \tag{9}$$

$$\text{Figure 4.} \quad Q_- = 5.20\, v^2 \times 10^{-8} \frac{\mu C}{min}, \tag{10}$$

The formulae (7) to (10) hold for all values of v. The ratio W_-/W_+ calculated from formulae (8) and (5) is

$$\text{Figure 16.} \quad \frac{W_+}{W_+} = 5.10\, v \times 10^{-3}, \quad v \geq 200 \frac{cc}{min} \tag{11}$$

The product $q_+ q_-$ calculated from formulae (6) and (9) is

$$\text{Figure 17.} \quad q_+ q_- = 64.4 \times v^2 \times 10^{-6} \frac{\mu C^2}{g}, \quad v \geq 200 \frac{cc}{min} \tag{12}$$

There is only one measurement below v = 200 cc/min. However, the functions in the region v < 200 cc/min can be constructued from this one measurement with good accuracy taking

$$\text{Figure 6.} \quad W_+ = 30\, v^2 \times 10^{-6} \frac{mg}{min}, \quad v \leq 200 \frac{cc}{min} \tag{13}$$

This together with the formula (7) for Q_+ gives

$$\text{Figure 10.} \quad q_+ = \frac{274}{v} \frac{\mu C}{g}, \quad v < 200 \frac{cc}{min} \tag{14}$$

The formula for q_+ can also be derived from the product $q_+ q_-$ shown in Figure 17.

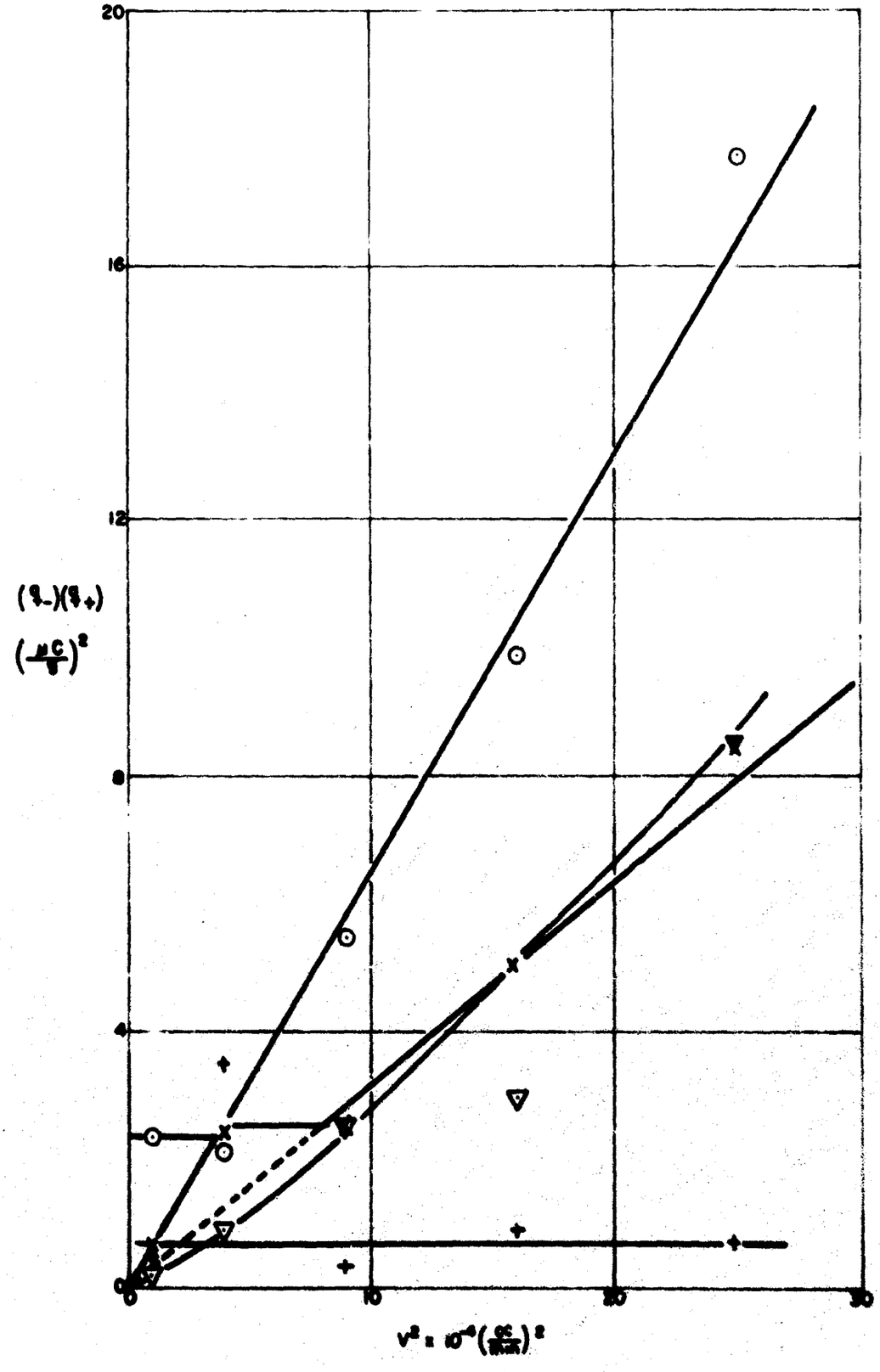

Figure 17. The product $q_+ \times q_-$ as a function of flow rate square v^2. ○ Saccharin, ✕ Saccharin + 1% Cab-O-Sil, ▽ Carbowax 6000 ▼ Carbowax 6000 + 1% Cab-O-Sil.

Below v = 200 cc/min this product is a constant,

$$\text{Figure 17.} \quad q_+ q_- = 2.4 \frac{\mu C^2}{g}, \; v < 200 \frac{cc}{min} \tag{15}$$

This divided by q_- from formula (9) gives

$$\text{Figure 10.} \quad q_+ = \frac{270}{v} \frac{\mu C}{g}, \; v < 200 \frac{cc}{min} \tag{16}$$

in aggrement with formula (14).

The ratio W_+ / W_- from formulae (13) and (8) is

$$\text{Figure 16.} \quad \frac{W_+}{W_-} = 5.14 \, v \times 10^{-3}, \; v \leq 200 \frac{cc}{min} \tag{17}$$

which is almost exactly the inverted value of that found at $v \geq 200$ cc/min according to formula (11). Thus, W_+/W_- increases proportionally to v up to $W_+ = W_-$, whereupon W_-/W_+ increases with v at the same rate. The measured value of W_-/W_+ given in Figure 16 for v = 100 cc/min is considerably lower than that given by formula (17), but the measured value for saccharin + 1% Cab-O-Sil coincides with the calculated values. This point will be further discussed below.

The product $P = Q_+ Q_-/W^2$ is plotted in Figure 18 The plot gives

$$\text{Figure 18.} \quad \frac{Q_+ Q_-}{W^2} = 0.140 \, v^2 \times 10^{-4} \; \frac{\mu C^2}{g}, \; v \geq 200 \tag{18}$$

$$\frac{Q_+ Q_-}{W^2} = 0.56, \; v < 200 \tag{19}$$

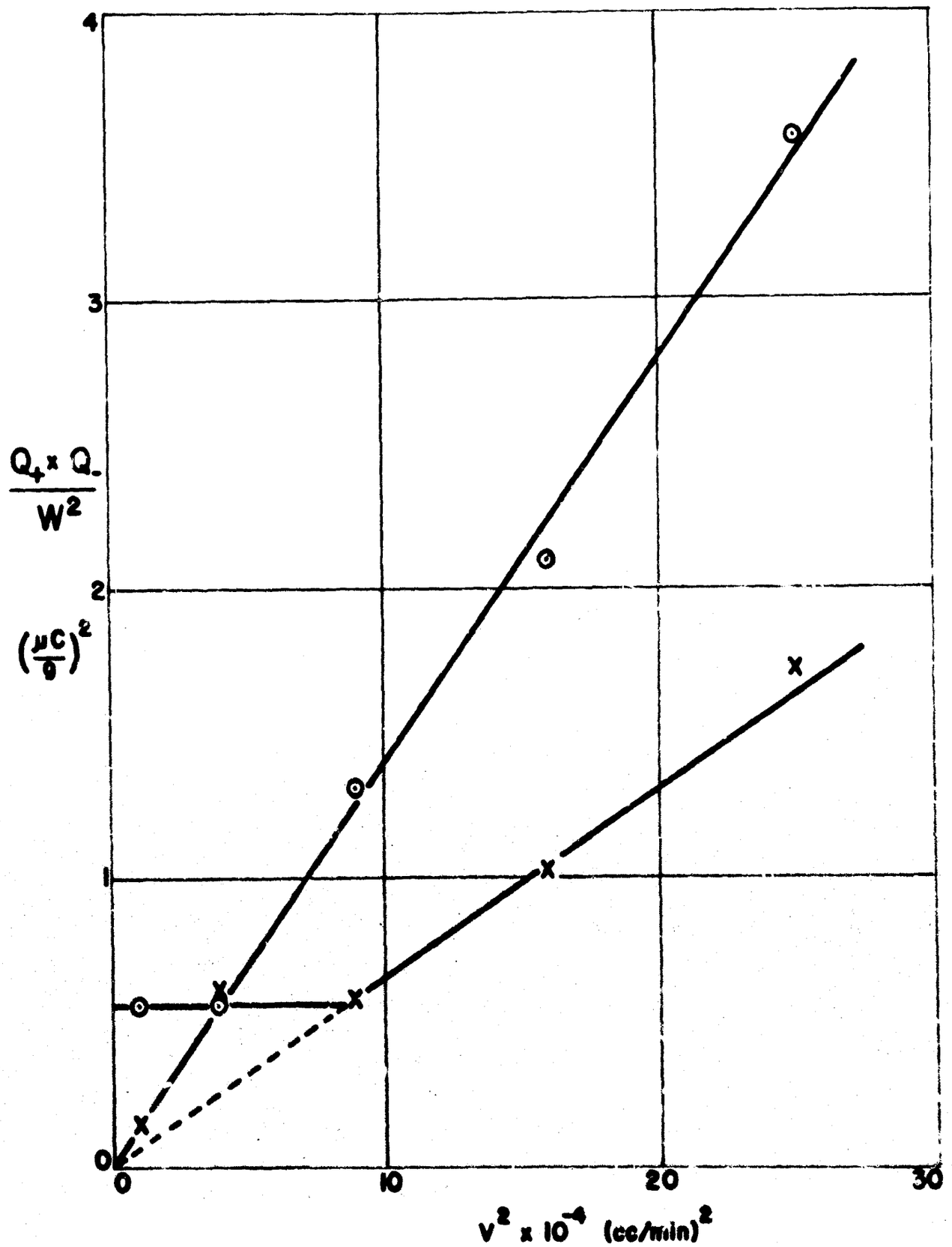

Figure 18. P = $Q_+ \times Q_- / W^2$ as a function of flow rate square v^2.
O Saccharin, X Saccharin + 1% Cab-O-Sil.

These two formulae together with the formulae (7) and (10) give

Figure 9. $$W = \left\{ \frac{Q_+ Q_-}{\frac{Q_+ Q_-}{W^2}} \right\}^{1/2} =$$

$$= 0.175\, v^{1/2} \frac{mg}{min}, \quad v \geq 200 \frac{cc}{min} \tag{20}$$

Figure 9. $$W = \left\{ \frac{Q_+ Q_-}{\frac{Q_+ Q_-}{W^2}} \right\}^{1/2} =$$

$$= 0.874\, v^{3/2} \times 10^{-3} \frac{mg}{min}, \quad v < 200 \frac{cc}{min} \tag{21}$$

These functions are plotted in Figure 9. They fit the data fairly well Of course, by definition, W is the sum of W_+ and W_-, and the formulae (20) and (21) are therefore approximate.

Finally, $q = Q_+ Q_-/W$ is shown in Figure 13. This plot is also linear. Using the formulae for Q_+, Q_-, W_+, and W_- we obtain

$$q = \frac{823\, v \times 10^{-8} + 5.20\, v^2 \times 10^{-8}}{1.14 \times 10^{-3} + 5.84\, v \times 10^{-6}} =$$

$$= 7.22 v \times 10^{-3} (1 + 1.20\, v \times 10^{-3}) \frac{\mu C}{g}, \quad v \geq 200 \frac{cc}{min} \tag{22}$$

$$q = \frac{823\, v \times 10^{-8} + 5.20\, v^2 \times 10^{-8}}{5.84\, v \times 10^{-6} + 30\, v^2 \times 10^{-9}} =$$

$$= 1.41 (1 + 1.18\, v \times 10^{-3}) \frac{\mu C}{g}, \quad v \geq 200 \frac{cc}{min} \tag{23}$$

These formulae agree with the data in Figure 13 by being linear and constant, respectively, but they differ in magnitudes and do not give a good fit. It appears that q is not a simple function of v for saccharin.

4.2 SACCHARIN + 1% CAB-O-SIL

The data for saccharin + 1% Cab-O-Sil are very similar in some respects to those for pure saccharin. The values of W_-/W_+ (Figure 16) differ less from the plot for saccharin than do the values for saccharin themselves. The values of $P = Q_+ Q_-/W^2$ (Figure 18) below $v = 200$ cc/min fall right on the curve for saccharin for $v \geq 200$ cc/min. The same applies to $q_+ q_-$ (Figure '7) and to q_+ (Figure 10). We may thus calculate q_- from $q_+ q_-$ and q_+ as given in formulae (12) and (6), respectively. This gives

$$\text{Figure 12.} \qquad q_- = 8.91\, v \times 10^{-3}\ \frac{\mu C}{g},\ v < 200\ \frac{cc}{min} \tag{24}$$

Thus, q_- for $v < 200$ cc/min follows the formula (9), which holds for saccharin at all values of v.

W_- is a constant between 200 and 300 cc/min

$$\text{Figure 8.} \qquad W_- = 3.32\ \frac{mg}{min},\ 100 \leq v \leq 200\ \frac{cc}{min} \tag{25}$$

We may thus calculate W_+ from W_+/W_- and W_- as given by formulae (17) and (25), respectively.

$$\text{Figure 6.} \qquad W_+ = 17.1\, v \times 10^{-3}\ \frac{mg}{min},\ v \leq 200\ \frac{cc}{min} \tag{26}$$

Combining the formulae (6) for q_+ and (26) for W_+ we obtain

$$\text{Figure 2.} \qquad Q_+ = q_+ W_+ = 12.3\, v^2 \times 10^{-8}\ \frac{\mu C}{min},$$

$$v \leq 200\ \frac{cc}{min} \tag{27}$$

Combining the formulae (24) for q_- and (25) for W_- we obtain

$$\text{Figure 4.} \qquad Q_- = q_- W_- = 0.296\, v \times 10^{-4} \frac{\mu C}{min},$$

$$v \leq 200 \frac{cc}{min} \tag{28}$$

As may be expected, the data for saccharin + 1% Cab-O-Sil scatter much more at high flow rates than do those for pure saccharin. Among the primary variables, Q_- shows comparatively little scatter.

$$\text{Figure 4.} \qquad Q_- = 17.8\, v^2 \times 10^{-8} \frac{\mu C}{min}, \quad v \geq 200 \frac{cc}{min} \tag{29}$$

The data for W (Figure 9) in the range $v \geq 200$ cc/min follow a straight line except for the point at v = 300 cc/min that is too high. This plot gives

$$\text{Figure 9.} \qquad W = 35.0\, v \times 10^{-3} \frac{mg}{min}, \quad v \geq 200 \frac{cc}{min} \tag{30}$$

W_- and W_+ are of the same order of magnitude in this range. Accordingly, they should both be proportional to v. The best straight lines on the data for W_- and W_+ are

$$\text{Figure 8.} \qquad W_- = 25.2\, v \times 10^{-3} \frac{mg}{min}, \quad v \geq 400 \frac{cc}{min} \tag{31}$$

$$\text{Figure 6.} \qquad W_+ = 10.0\, v \times 10^{-3} \frac{mg}{min}, \quad v \geq 400 \frac{cc}{min} \tag{32}$$

These add up to the formula (30) for W.

The data for $P = Q_+ Q_- / W^2$ in Figure 18 fall on a straight line

$$\text{Figure 18.} \qquad \frac{Q_+ Q_-}{W^2} = 656\, v^2 \times 10^{-8} \left(\frac{\mu C}{g}\right)^2, \quad v \geq 300 \frac{cc}{min} \tag{33}$$

This gives us a formula for Q_+, inserting Q_- and ' from formulae (29) and (30), respectively,

Figure 2. $$Q_+ = 4.52\, v^2 \times 10^{-8}\, \frac{\mu C}{min}, \quad v \geq 300\, \frac{cc}{min} \tag{34}$$

Dividing by W_+ from formula (32) we obtain

Figure 10. $$q_+ = 4.52\, v \times 10^{-3}\, \frac{\mu C}{g}, \quad v \geq 300\, \frac{cc}{min} \tag{35}$$

The fit is much better than that for Q_+ since the density variations are eliminated.

From the formulae (29) and (31) we obtain

Figure 12. $$q_- = \frac{Q_-}{W_-} = 7.06\, v \times 10^{-3}\, \frac{\mu C}{g}, \quad v \geq 300\, \frac{cc}{min} \tag{36}$$

From formulae (35) and (36) we obtain

Figure 17. $$q_+ q_- = 31.9\, v^2 \times 10^{-6} \left(\frac{\mu C}{g}\right)^2, \quad v \geq 300\, \frac{cc}{min} \tag{37}$$

Among the plots of the charge data it is really only q_- that shows a poor fit with the data. This is associated with the poor fit for the data for W_-.

It now remains to join the curves for low and for high values of v. We see then from Figures 10 and 17 that q_+ and $q_+ q_-$ are constant. Furthermore, $Q_+ Q_-/W^2$ is a constant but Q_- is proportional to v^2 and W to v. Hence, Q_+ is a constant. Consequently W_+ is a constant. Since Q_- is proportional to v^2 and q_- is constant, W_- is proportional v^2. The function

Figure 8. $$W_- = 0.41\, v^2 \times 10^{-4}\, \frac{mg}{min}, \quad 200 \leq v \leq 300\, \frac{cc}{min} \tag{38}$$

connects the two branches of the curve at low and at high flow rates.

The data discussed above and presented in Section 3 are those from a second run. The data for the first run sometimes come out bad because the coat on the tube wall may not be well built up. However, the data from the first run shed some light on the scatter of the data and thereby upon the effect of the deagglomerant. They are therefore given in this section.

The data for the weights (Figure 19) all show breaks at v = 200 cc/min. Figure 20 shows W_-/W_+. The curves drawn are according to formulae (11) and (17).

In this case Q_+ and W_+ are

$$\text{Figure 21.} \qquad Q_+ = 2.16\, v \times 10^{-5}\ \frac{\mu C}{\text{min}} \tag{39}$$

$$\text{Figure} \qquad W_+ = 4\ \frac{mg}{\text{min}}, \quad v \geq 200\ \frac{cc}{\text{min}} \tag{40}$$

This gives with formula (38)

$$\text{Figure 22.} \qquad q_+ = \frac{Q_+}{W_+} = 5.04\, v \times 10^{-3}\ \frac{\mu C}{g}, \quad v \geq 200\ \frac{cc}{\text{min}} \tag{41}$$

which is about 10% higher than that given in formula (35).

At low flow rates

$$\text{Figure 19.} \qquad W_+ = v^2 \times 10^{-4}\ \frac{mg}{\text{min}}, \quad v \leq 200\ \frac{cc}{\text{min}} \tag{42}$$

This gives with formula (39)

$$\text{Figure 22.} \qquad q_+ = \frac{Q_+}{W_+} = \frac{216}{v}, \quad v \leq 200\ \frac{cc}{\text{min}} \tag{43}$$

This is similar to the formula (16) for saccharin. The observed value at v = 100 cc/min falls far below this curve.

4.3 CAB-O-SIL

The data for Cab-O-Sil that scatter least are those for q_- and Q_-

$$\text{Figure 12.} \qquad q_- = 49.9\, v \times 10^{-3}\ \frac{\mu C}{g} \tag{44}$$

$$\text{Figure 4.} \qquad Q_- = 2.53\, (v - 35) \times 10^{-4}\ \frac{\mu C}{\text{min}} \tag{45}$$

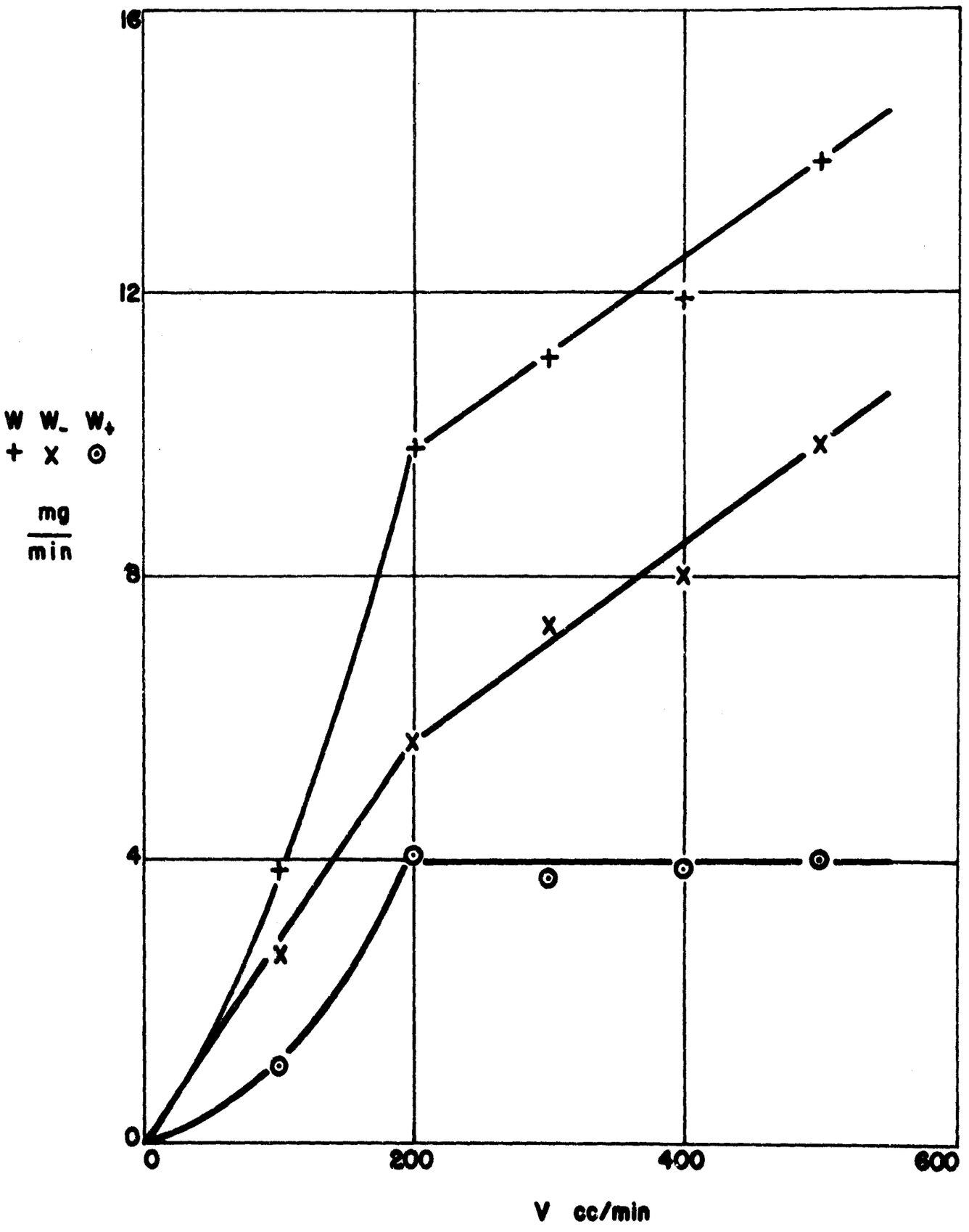

Figure 1 . Weights of positive deposit in 1 min W_+, negative deposit W_-, and sum of positive and negative deposits $W = W_+ + W_-$ as functions of flow rate v for the first run of Saccharin + 1% Cab-O-Sil. + W_+, × W_-, + W.

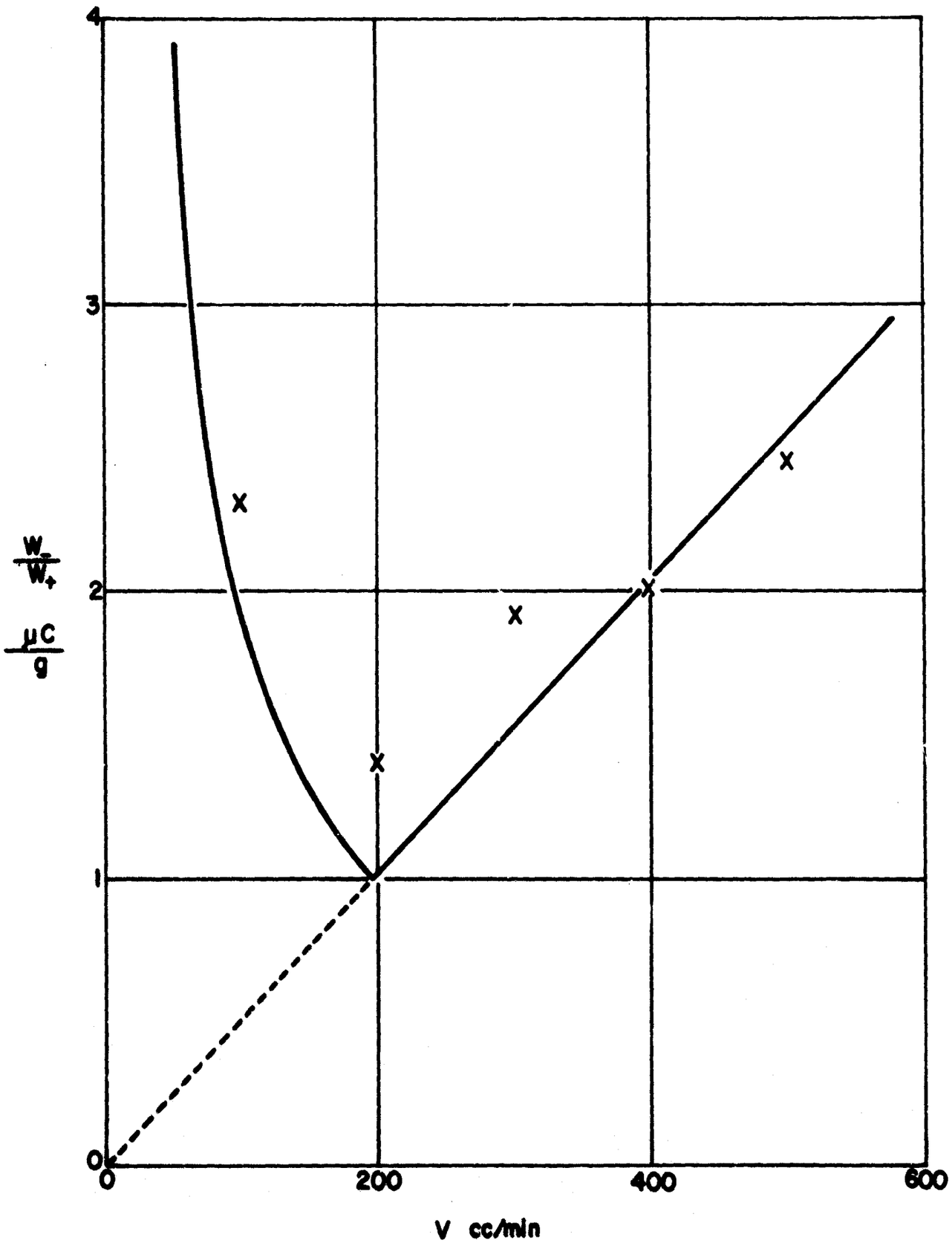

Figure 20. Ratio of weights of ;negative and positive deposits in 1 min W_-/W_+ as a function of flow rate v for the first run of Saccharin + 1% Cab-O-Sil.

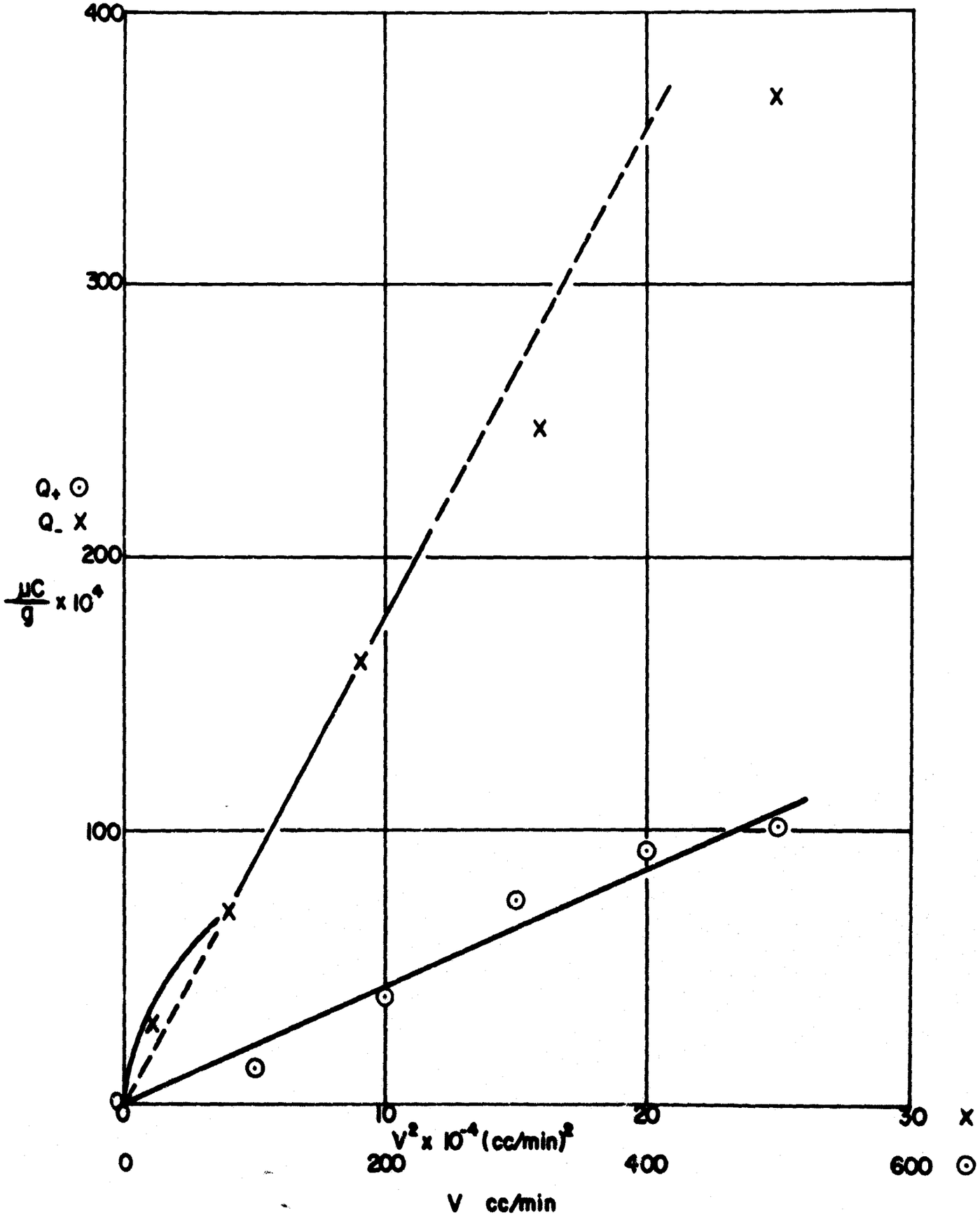

Figure 21. Total po itive charge Q_+ and total negative charge Q_- deposited in 1 min as functions of flow rate v and square of flow rate v^2, respectively, for the first run of Saccharin + 1% Cab-O-Sil.

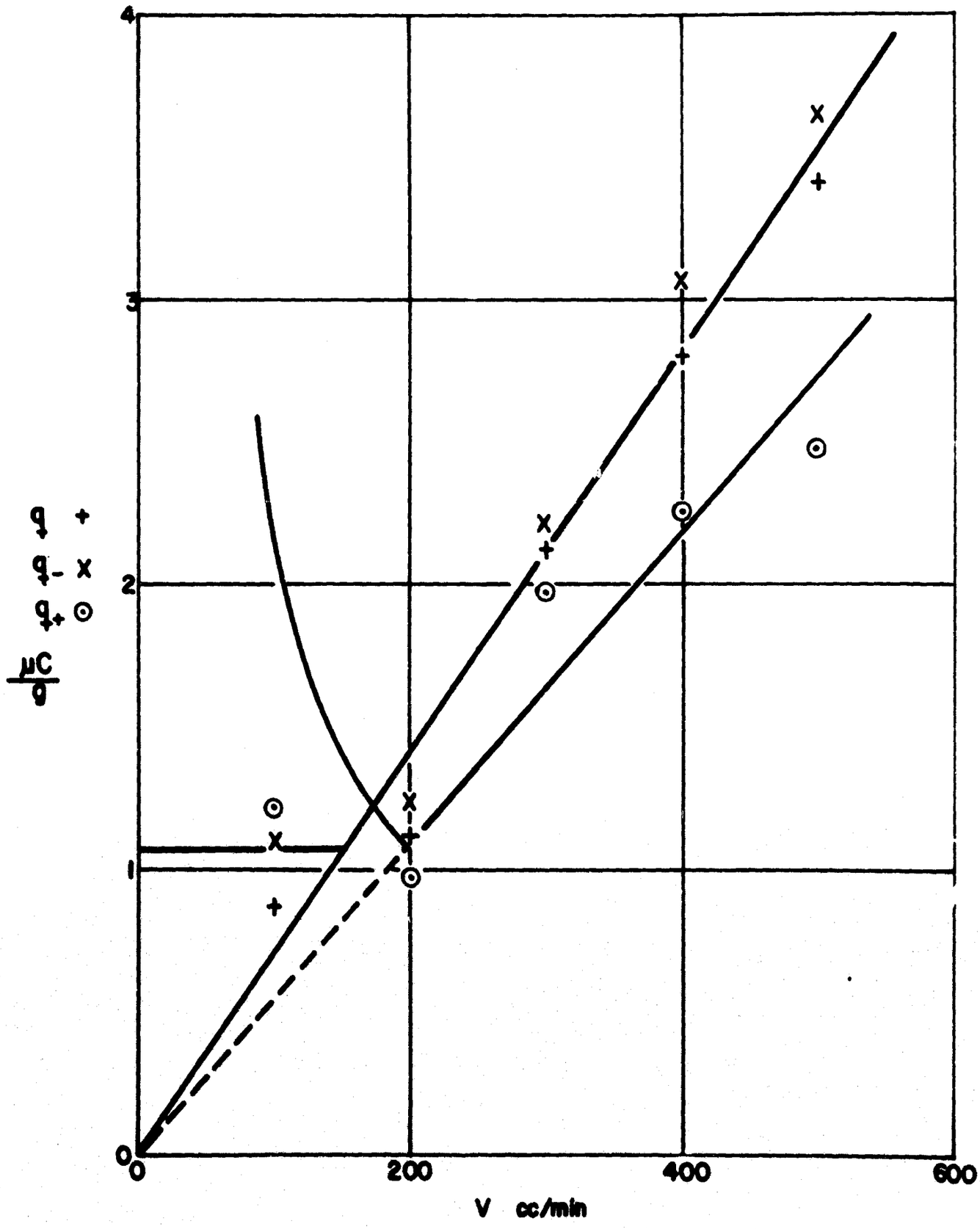

Figure 22. Average charge per gram of positive deposit q_+, negative deposit q_-, and absolute charge q as functions of flow rate v for the first run of Saccharin + 1% Cab-O-Sil, q_+, X q_-, + q.

These formulae give

$$\text{Figure 8.} \qquad W_- = \frac{Q_-}{q_-} = 5.07\ (1 - \frac{35}{v}) \times 10^3 \frac{mg}{min} \tag{46}$$

At high flow rates, W_+ is a constant

$$\text{Figure 7.} \qquad W_+ = 0.183 \frac{mg}{min}, \quad v \geq 300 \frac{cc}{min} \tag{47}$$

Assuming that Q_+ is proportional to v^2

$$\text{Figure 3.} \qquad Q_+ = 18.8\, v^2 \times 10^{-8} \frac{\mu C}{min}, \quad v \geq 200 \frac{cc}{min} \tag{48}$$

we have

$$\text{Figure 11.} \qquad q_+ = \frac{Q_+}{W_+} = 1.05\, v^2 \times 10^{-3} \frac{\mu C}{g},$$

$$v \geq 300 \frac{cc}{min} \tag{49}$$

Formulae (49) and (44) give

$$\text{Figure 23.} \qquad q_+ q_- = 52\, v^3 \times 10^{-6} \frac{\mu C}{g}, \quad v \geq 200 \frac{cc}{min} \tag{50}$$

Formulae (48), (45), (47), and (46) give

$$\text{Figure 24.} \qquad \frac{Q_+ Q_-}{W^2} = 1.90 \frac{v^4}{v-35} \times 10^{-6} \left(\frac{\mu C}{g}\right)^2, \quad v \geq 200 \frac{cc}{min} \tag{51}$$

At small values of v,

$$\text{Figure 7.} \qquad W_+ = 2.35\, v \times 10^{-3} \frac{mg}{min}, \quad v \geq 200 \frac{cc}{min} \tag{52}$$

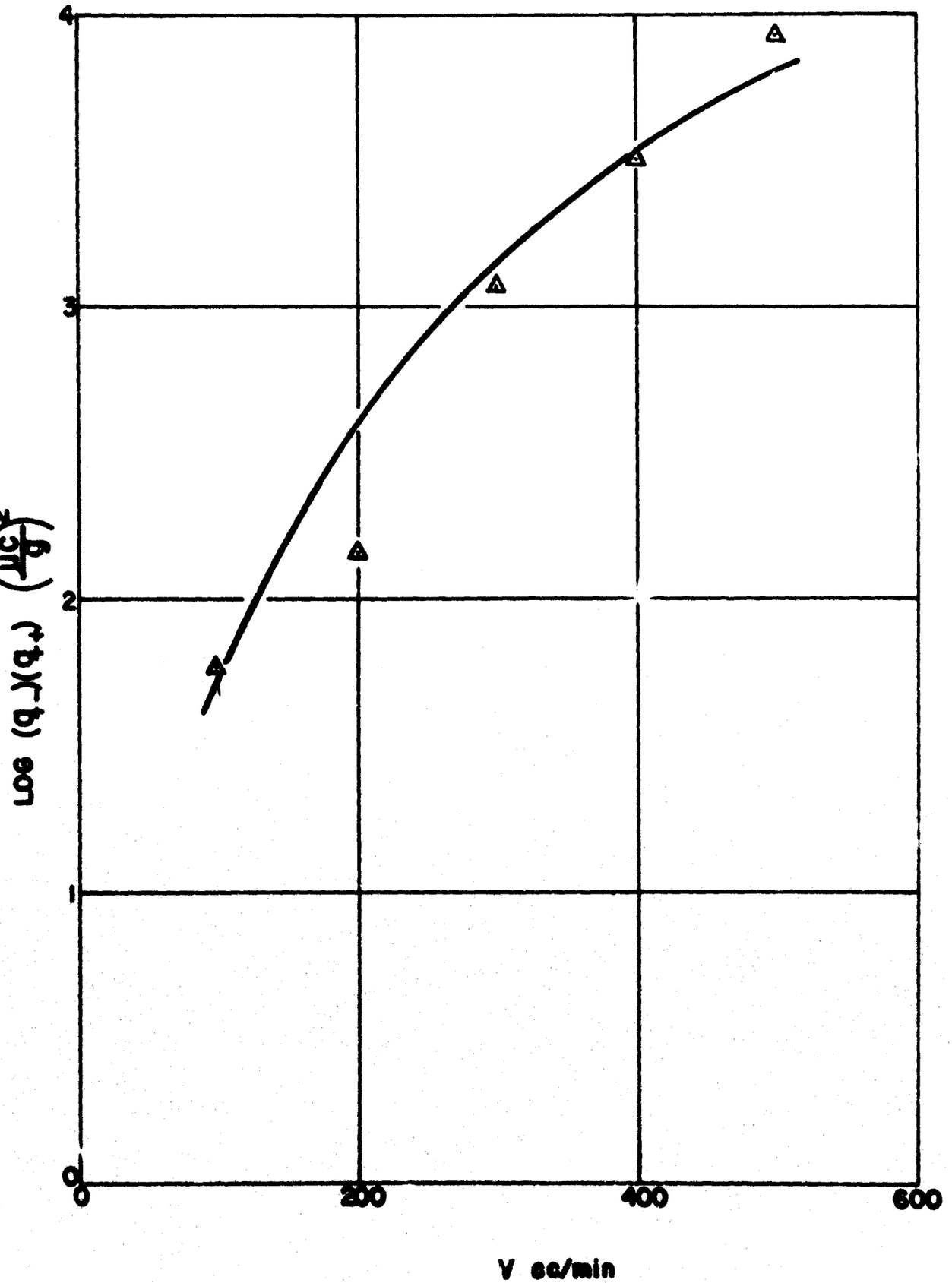

Figure 23. Logarithm of the product $q_+ \times q_-$ as a function of flow rate v for Cab-O-Sil.

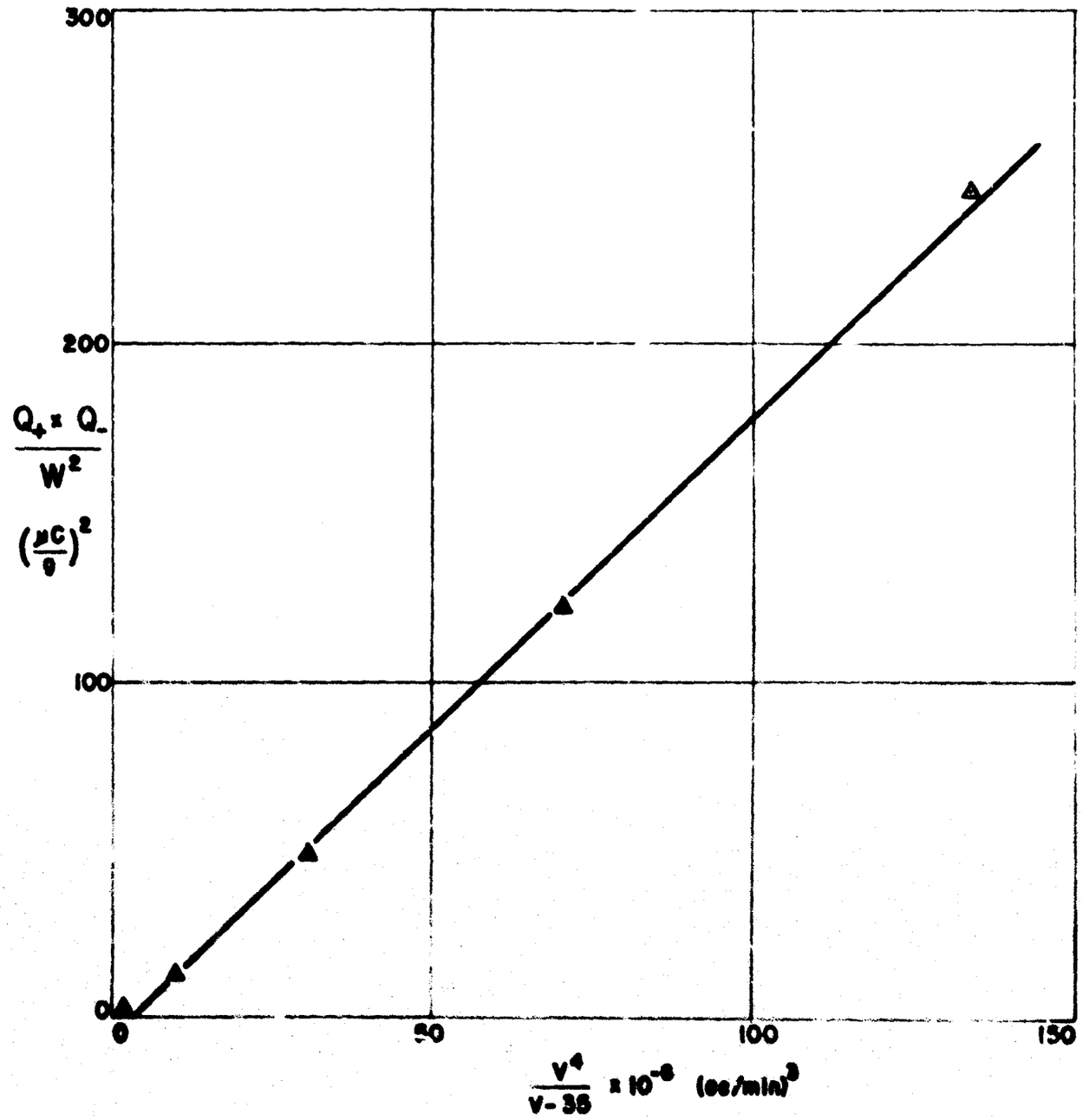

Figure 24. $P_4 = Q_+ \times Q_-/W^2$ as a function of $v^4/v-35$ for Cab-O-Sil.

This gives with formula (46)

$$\text{Figure 16.} \quad \frac{W_-}{W_+} = \frac{2120}{v}\left(1 - \frac{35}{v}\right), \quad v \leq 200 \ \frac{cc}{min} \tag{53}$$

The data at small values of v are difficult to interpret, but below $v = 35$ cc/min, $Q_- = 0$ and $W_- = 0$ so that $q_+ q_-$ and $Q_+ Q_-/W^2$ are both zero.

At high values of v, formulae (46) and (47) give

$$\text{Figure 16} \quad \frac{W_-}{W_+} = 27.7\left(1 - \frac{35}{v}\right), \quad v > 300 \ \frac{cc}{min} \tag{54}$$

At small values of v,

$$\text{Figure 3.} \quad Q_+ = 0.33\, v \times 10^{-4} \ \frac{\mu C}{min}, \quad v \leq 200 \ \frac{cc}{min} \tag{55}$$

The formulae (55) and (52) give

$$\text{Figure 11.} \quad q_+ = \frac{Q_+}{W_+} = 14 \ \frac{\mu C}{g}, \quad v \leq 200 \ \frac{cc}{min} \tag{56}$$

in fair agreement with the data.

Formulae (56) and (44) give

$$\text{Figure 23.} \quad q_+ q_- = 0.7\, v \left(\frac{\mu C}{g}\right)^2, \quad v \leq 200 \ \frac{cc}{min} \tag{57}$$

Above $v = 50$ cc/min, W_- is much larger than W_+. We may then take $W = W_-$ and obtain from formulae (55), (45), and (46)

$$\text{Figure 24.} \quad \frac{Q_+ Q_-}{W^2} = \frac{3.25\, v^3}{v - 35} \times 10^{-4}, \quad 50 < v \leq 200 \ \frac{cc}{min} \tag{58}$$

4.4 CARBOWAX 6000

The data for q give a very good straight line, which indicates a high degree of accuracy in the measurements.

$$\text{Figure 14.} \qquad q = 4.30\ v \times 10^{-3}\ \frac{\mu C}{g} \tag{59}$$

Q_+ and W_+ are both very large as compared to Q_- and W_-, and q is therefore essentially equal to q_+ at high flow rates.

$$\text{Figure 10.} \qquad q_+ = 4.18\ v \times 10^{-3}\ \frac{\mu C}{g} \tag{60}$$

In order that q and q_+ be proportional to v, Q and Q_+ should be proportional to v^2, and W and W_+ to v. The scatter in these data is very bad, but Q_+ gives a reasonably straight line against v^2,

$$\text{Figure 3.} \qquad Q_+ = 3.05\ v^2 \times 10^{-8}\ \frac{\mu C}{min} \tag{61}$$

Hence, from formulae (61) and (60)

$$\text{Figure 7.} \qquad W_+ = \frac{Q_+}{q_+} = 7.30\ v \times 10^{-3}\ \frac{mg}{min} \tag{62}$$

The data for q_- give

$$\text{Figure 12.} \qquad q_- = 10.25\ (v - 90) \times 10^{-3}\ \frac{\mu C}{min} \tag{64}$$

A similar plot fits the data for Q_-

$$\text{Figure 5.} \qquad Q_- = 123\ (v - 90) \times 10^{-8}\ \frac{\mu C}{min} \tag{64}$$

Hence, from formulae (64 and (63)

$$\text{Figure 8.} \qquad W_- = \frac{Q_-}{q_-} = 0.120\ \frac{mg}{min} \tag{65}$$

The data indicate the W_- is constant and give roughly

$$W_- = 0.12 \tag{66}$$

From formulae (62) and (65) we obtain

$$\frac{W_+}{W_-} = 0.0609\ v \tag{67}$$

The data may indicate

Figure 15. $$\frac{W_+}{W_-} = 0.024\ v \tag{68}$$

There is a difference by a factor of 2.5 in the two formulae, but formula (67) is probably more accurate.

4.5 CARBOWAX 6000 + 1% CAB-O-SIL

The data for the weights scatter remarkably little

Figure 9. $$W = 50\ v \times 10^{-3}\ \frac{mg}{min},\quad v \geq 200\ \frac{cc}{min} \tag{69}$$

Figure 7. $$W_+ = 31\ v \times 10^{-3}\ \frac{mg}{min},\quad v \geq 200\ \frac{cc}{min} \tag{70}$$

The difference is

Figure 8. $$W_- = W - W_+ = 19\ v \times 10^{-3}\ \frac{mg}{min},\quad v \geq 200\ \frac{cc}{min} \tag{71}$$

A straight line for q_+ gives

Figure 10. $$q_+ = 2.22\ v \times 10^{-3}\ \frac{\mu C}{g},\quad v > 200\ \frac{cc}{min} \tag{72}$$

Formulae (72) and (70) give

$$\text{Figure 3.} \qquad Q_+ = q_+ W_+ = 6.88\, v^2 \times 10^{-8} \frac{\mu C}{min}, \quad v > 200 \frac{cc}{min} \tag{73}$$

The data for q_- (Figure 12) suggest that q_- is a constant and that therefore, since W_- is proportional to v, Q_- is proportional to v. On the other hand, the data for $q_+ q_-$ (Figure 17) indicate that $q_+ q_-$ is a constant and therfore, since q_+ is proportional to v, that q_- is proportional to v^{-1} and Q_- a constant. Adopting the latter alternative we find

$$\text{Figure 4.} \qquad Q_- = 7.0 \times 10^{-3} \frac{\mu C}{min}, \quad v > 300 \frac{cc}{min} \tag{74}$$

and from formulae (74) and (71)

$$\text{Figure 12.} \qquad q_- = \frac{Q_-}{W_-} = \frac{368}{v} \frac{\mu C}{g}, \quad v \geq 200 \frac{cc}{min} \tag{75}$$

It appears that the value of Q_- measured at v = 300 cc/min is off by a factor of approximately 3 and that q_- therefore is off by the same amount.

Formulae (72) and (75) give

$$\text{Figure 17.} \qquad q_+ q_- = 0.82 \frac{\mu C}{g}, \quad v \geq 200 \frac{cc}{min} \tag{76}$$

The average of the measured values is 0.7 μC/g, but this average includes the low value at v = 300 cc/min. If this value is disregarded, the average is 0.8 μC/g, in agreement with the calculated value.

Formulae (73), (74), and (69) give

$$\text{Figure 25.} \qquad \frac{Q_+ Q_-}{W^2} = 0.19 \frac{\mu C}{g}, \quad v > 200 \frac{cc}{min} \tag{77}$$

This is in agreement with the data.

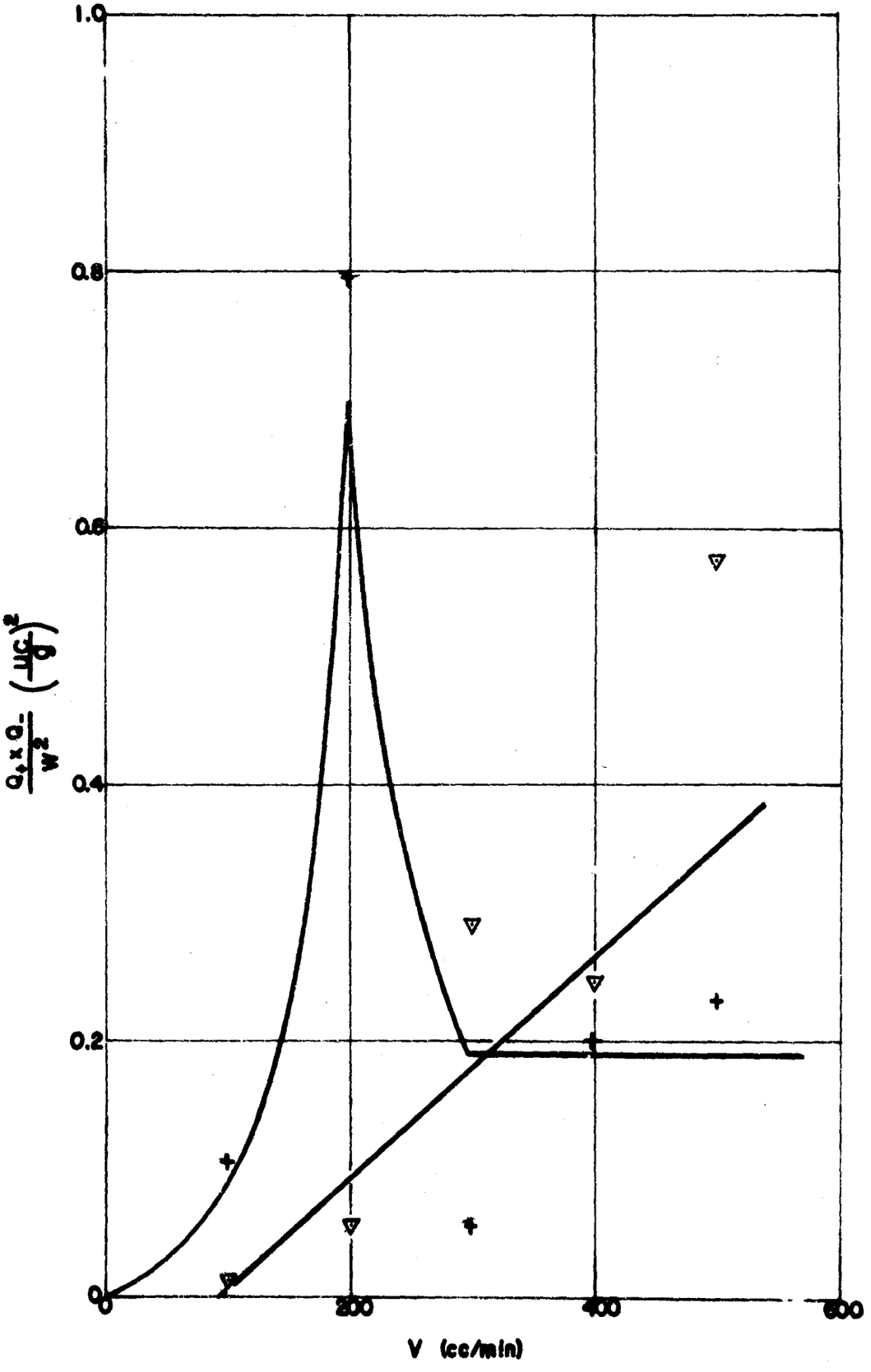

Figure 25. $P = Q_+ \times Q_- / W^2$ as a function of flow rate v. ▽ Carbowax 6000, + Carbowax 6000 + 1% Cab-O-Sil.

The formulae (70) and (71) give

$$\text{Figure 15.} \quad \frac{W_+}{W_-} = 1.63, \quad v \geq 200 \frac{cc}{min} \tag{78}$$

At low flow rates, q_- appears to be proportional to v^2,

$$\text{Figure 12.} \quad q_- = 0.45\, v^2 \times 10^{-4} \frac{\mu C}{g}, \quad v \leq 200 \frac{cc}{min} \tag{79}$$

This gives $q_- = 1.80\ \mu C/g$ at $v = 200$ cc/min. Formulae (75) gives $q_- = 1.84\ \mu C/g$ at $v = 200$ cc/min. Thus, the functions (75) and (79) intersect at $v = 200$ cc/min. q_+ is proportional to v,

$$\text{Figure 10.} \quad q_+ = 8.0\, v \times 10^{-3} \frac{\mu C}{g}, \quad v \leq 200 \frac{cc}{min} \tag{80}$$

Formulae (80) and (79) give

$$\text{Figure 17.} \quad q_+ q_- = 0.36\, v^3 \times 10^{-6} \left(\frac{\mu C}{g}\right)^2, \quad v \leq 200 \frac{cc}{min} \tag{81}$$

The measured values at $v = 100$ cc/min are $q_+ = 0.8\ \mu C/g$ and $q_- = 0.45\ \mu C/g$ and, thus, $q_+ q_- = 0.36\ (\mu C/g)^2$. The corresponding values at $v = 200$ cc/min are $q_+ = 1.53\ \mu C/g$ and $q_- = 2.35\ \mu C/g$. If the latter value is replaced by that given by formulae (75) and (79) i.e., $q_- = 1.8\ \mu C/g$, the product is $q_+ q_- = 2.8\ (\mu C/g)^2$ which is not far off the value $q_+ q_- = 2.9\ (\mu C/g)^2$ calculated from formula (81).

The values of W at $v = 100$ and $v = 200$ cc/min are 1.25 and 10 mg/min, respectively. Hence,

$$\text{Figure 9.} \quad W = 1.25\, v^3 \times 10^{-6} \frac{mg}{min}, \quad v \leq 200 \frac{cc}{min} \tag{82}$$

A similar formula holds for W_+

$$\text{Figure 7.} \quad W_+ = 0.75\, v^3 \times 10^{-6} \frac{mg}{min}, \quad v \leq 200 \frac{cc}{min} \tag{83}$$

Hence,

$$\text{Figure 8.} \qquad W_- = W - W_+ = 0.50\, v^3 \times 10^{-6} \frac{mg}{min},$$

$$v \leq 200 \frac{cc}{min} \tag{84}$$

Formulae (83) and (84) give

$$\text{Figure 15.} \qquad \frac{W_+}{W_-} = 1.50, \quad v \leq 200 \frac{cc}{min} \tag{85}$$

Formulae (80) and (83) give

$$\text{Figure 3.} \qquad Q_+ = q_+ W_+ = 6.0\, v^4 \times 10^{-12} \frac{\mu C}{min},$$

$$v \leq 200 \frac{cc}{min} \tag{86}$$

in agreement with the measured value, $Q_+ = 96 \times 10^{-4}$ μC/min at v = 200 cc/min.

Formulae (79) and (84) give

$$\text{Figure 5.} \qquad Q_- = q_- W_- = 2.25\, v^5 \times 10^{-14} \frac{\mu C}{min},$$

$$v \leq 200 \frac{cc}{min} \tag{87}$$

This gives $Q_- = 2.25 \times 10^{-4}$ μC/min at v = 100 cc/min in fair agreement with the observed value 2.67×10^{-4}. The formula (87) gives $Q_- = 71 \times 10^{-4}$ μC/min at v = 200 cc/min which is about 20% lower than the observed value 86.2×10^{-4}. It is obvious that a small error in v with such a steep curve causes a great error in Q_-. The observed value $Q_- = 86.5$ corresponds according to formula (87) to v = 208 cc/min.

Formulae (86), (87), and (82) give

$$\text{Figure 25.} \quad \frac{Q_+ Q_=}{W^2} = 8.65\, v^3 \times 10^{-8} \left| \frac{\mu C}{g} \right|^2, \quad v \leq 200 \frac{cc}{min} \qquad (88)$$

The function Q_- can be constructed from formulae (75) and (71) in the interval 200-300 cc/min, because both formulae are valid in this entire range. Thus, the formula (74) holds for $v \geq 200$ cc/min. The true value of Q_- at $v = 200$ cc/min is thus somewhere between 70×10^{-4} and 72×10^{-4} μC/min as calculated from formulae (74) and (87), respectively. The measured value, $Q_- = 86.5 \times 10^{-4}$ μC/min is probably too high.

Neither Q_+ nor q_+ permit extension in the range 200 - 300 cc/min. However, the ratio between the values of q_+ at $v = 200$ and $v = 300$ cc/min is 15.3/6.7 = 2.28, which is close to $(3/2)^2 = 2.25$. This suggests that

$$\text{Figure 10.} \quad q_+ = \frac{6.1}{v^2} \times 10^4 \frac{\mu C}{g}, \quad 200 \leq v \leq 300 \frac{cc}{min} \qquad (89)$$

The formulae (89) and (70) give

$$\text{Figure 3.} \quad Q_+ = q_+ W_+ = \frac{1.89}{v} \frac{C}{min},$$

$$200 \leq v \leq 300 \frac{cc}{min} \qquad (90)$$

5. AGGLOMERATION IN POWDERS AND AEROSOLS

It was shown in preceding investigations [3, 4, 7] that adhesion between powder particles is caused by electrostatic forces at low humidities and by hydrogen bonds with water at higher humidities. The limit is

at 4% RH for silica sand[3] and at 7% RH for plexiglass[4]. It is difficult to handle fine powders at high humidities, and, in practice, dry powders for aerosol production will be held at some technically achievable low humidity. In the work of Nash et al[5] in this field, the relative humidity was held at 2%. It appears that a still lower humidity, say, 0.5% RH, would be preferable and also attainable.

It was shown in other preceding investigations[8, 9] that collisions between aerosol particles are determined by electrostatic forces. Oppositely charged particles collide as a result of electrostatic attraction, particles of equal polarity are prevented from colliding by electrostatic repulsion. This holds at all humidities of the air.

The data presented in Section 2 were obtained at a comparatively high humidity, 10%. They apply directly to collisions in aerosols sprayed at 10% RH. They also apply directly to agglomeration in powders, for which electrostatic adhesion predominates at 10% RH. They apply indirectly to agglomeration in powders at lower humidities on the assumption that the charge distribution is essentially the same at the lower humidities, whereas the charge level may be higher at the lower humidities. The data will be discussed on this basis in this section and in Section 6.

Agglomeration may be discussed in terms of forces of adhesion within the agglomerates and the number of particles engaged in agglomerates. At low humidities, the former quantity is determined essentially by the magnitude of the charge; the latter quantity is determined essentially by the charge distribution. In the cases under consideration there were no neutral particles. Hence, agglomeration occurs with oppositely charged particles only.

The number of particles engaged in agglomerates, ν, may be expressed in terms of W_+ / W_-. When this quantity is zero or infinite, i.e., for unipolar charge, there are no agglomerates, and ν is therefore zero for these two values of W_+ / W_-. When $W_+ / W_- = 1$, all the particles may be engaged in agglomerates, and ν has therefore a maximum at $W_+ / W_- = 1$.

As the size of an agglomerate increases, the external forces acting upon it also increase. It is conceivable that the agglomerate grows by addition of particles of successively smaller charges. The size of the agglomerates should thus be determined by the force of adhesion

and, therefore, by the magnitude of the charge or, specifically, by the product of the magnitudes of the positive and negative charges per particle. A rough estimate of the force of adhesion may be given by the product of q_+ and q_-.

One may thus consider a "degree of agglomeration" determined by the two quantities W_+/W_- and $q_+ q_-$. Figure 26 shows a schematic representation of the "degree of agglomeration" as a function of W_+/W_- for various values of $q_+ q_-$ in arbitrary units.

These considerations hold equally for the two cases, agglomeration in milling, handling, and slow flow, and agglomeration in aerosols. But in the latter case, we may also consider the rate of agglomeration. This quantity is determined by the long-range electrostatic forces between the particles and by the density of the aerosol. If the numbers of positive and negative particles per unit volume are n_+ and n_-, respectively, and the total number of particles per unit volume is $n = n_+ + n_-$, the average distance between particles is $1/n$. At a random distribution $q_+ q_-/n^2$ thus gives a measure of the force of attraction between positive and negative particles. The frequency of collisions and thereby the rate of agglomeration may thus be expressed in terms of

$$P = q_+ q_- \frac{n_+ n_-}{n^2}$$

But $q_+ n_+ = Q_+^1$ and $q_- q_- = Q_-^1$ are the total positive and negative charges per unit volumes, and Q_+^1/n and Q_-^1/n are proportional to the positive and negative charges per gram of aerosol material. Hence,

$$P = \frac{Q_+ Q_-}{W^2}$$

disregarding a conversion factor and using the notations previously introduced.

The quantities $q_+ q_-$ and $P = Q_+ Q_-/W^2$, are plotted in Figures 18, 24 and 25.

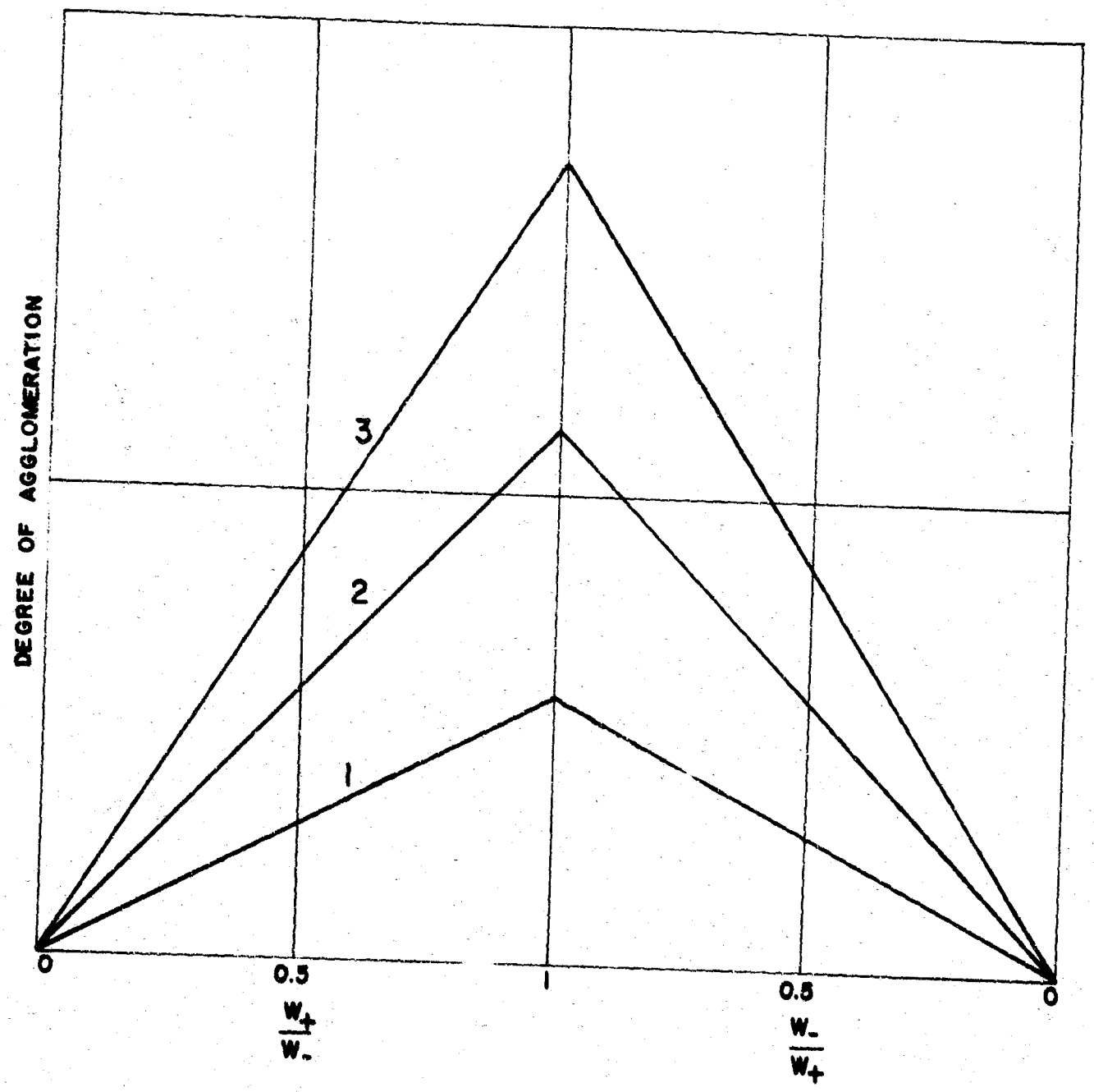

Figure 26. Schematic representation of "degree of agglomeration" as a function of the ratios W_+/W_- and W_-/W_+ at different values of the product $q_+ \times q_-$.

An attempt at a concise presentation of the data is offered in Tables 1 and 2, showing the data at lo and at high flow rates, respectively. Unfortunately, not all the plots permit simple analytical expressions. Nevertheless, the data given in Tables 1 and 2 assist in the comparison between the powders and in the evaluation of the deagglomerant, but the actual plots should be consulted for additional information.

6. DISCUSSION

Since agglomeration was not studied directly the conclusions drawn from the data are necessarily tentative and subject to checking by direct observation. Furthermore, in spite of the inherent accuracy of the measurements, there are some large deviations, occasionally by a factor of 3, in the data that are difficult to account for and that also need checking.

However, the information that this investigation was planned to provide is sufficiently accurate for safe conclusions. The agglomeration factors discussed in Section 5 are all ratios, e.g., W_-/W_+. These ratios do not depend upon the density of the aerosol in the aerosol generator. They have been calculated from the data and from the formula derived in Section 4 at $v = 50$ and $v = 500$ cc/min. They are listed in Table 3.

The aerosol in the aerosol generator contains very little of small particles. Most of the aerosol particles are agglomerates of the powder particles. The data in Table 3 pertain to these agglomerates and to the agglomeration of these agglomerates.

Comparing the data for saccharin and saccharin + 1% Cab-O-Sil it is apparent that the deagglomerant has no effect upon W_-/W_+ but that it reduces q_+q_- and $P = Q_+Q_-/W^2$, at low flow rates considerably, at high flow rates slightly. Thus, the deagglomerant is effective at low flow rates but ineffective at high flow rates. It reduces the strength of the agglomerates by a factor of 15 at $v = 50$ cc/min but only by a factor of 2 at $v = 500$ cc/min. It reduces the probability of collisions in the aerosol by a factor of 15 at $v = 50$ cc/min but only by a factor of 2 at $v = 500$ cc/min. Since the spraying of aerosols occurs at high flow rates, it follows that the deagglomerant has no effect upon agglomeration in sprayed aerosols, although it is effective in promoting free flow at low flow rates.

Comparing the data for Carbowax 6000 and Carbowax 6000 + 1% Cab-O-Sil we find a drastic change to the worse in the factor W_+/W_-. In the pure material there are only positive particles (or agglomerates)

	Saccharin	Saccharin + 1% Cab-O-Sil	Carbowax 6000	Carbowax 6000 + 1% Cab-O-Sil	Cab-O-Sil
$Q_+ \frac{\mu C}{min} \times 10^8$	$823\ v$	$12.3\ v^2$	$3.05\ v^2$	$6.0\ v^4 \times 10^{-4}$	$3.300\ v$
$Q_- \frac{\mu C}{min} \times 10^8$	$5.20\ v^2$	$2960\ v$	$123\ (v - 90)$	$2.25\ v^5 \times 10^{-6}$	$2.53\ (v - 35) \times 10^4$
$W_+ \frac{\mu g}{min}$	$30\ v^2 \times 10^{-3}$	$17.1\ v$	$7.30\ v$	$0.75\ v^3 \times 10^{-3}$	$2.35\ v$
$W_- \frac{\mu g}{min}$	$5.84\ v$	$33\ v$	123	$0.50\ v^3 \times 10^{-3}$	$5.07\ (1 - \frac{35}{v}) \times 10^3$
$W \frac{\mu g}{min}$	$0.874\ v^{3/2}$	$50\ v$		$1.25\ v^3 \times 10^{-3}$	
$q_+ \frac{\mu C}{g} \times 10^3$	$\frac{274}{v}$	$7.22\ v$	$4.18\ v$	$8.0\ v$	14×10^3
$q_- \frac{\mu C}{g} \times 10^3$	$8.91\ v$	8.91	$10.25\ (v - 90)$	$0.045\ v^2$	$49.9\ v$
$W_+ / W_- \times 10^3$	$5.14\ v$	$5.14\ v$	$60.9\ v \times 10^{-3}$		
W_- / W_+					$\frac{2120}{v}\ (1 - \frac{35}{v})$
$q_+ q_- (\frac{\mu C}{g})^2 \times 10^6$	2.4×10^6	$64.4\ v^2$	$42.7\ v\ (v - 90)$	$0.36\ v^3$	$0.7\ v \times 10^6$
$\frac{Q_+ Q_-}{W^2} (\frac{\mu C}{g})^2 \times 10^4$	0.56×10^4	$0.140\ v^2$	$8.7\ (v - 90)$	$8.65\ v^3 \times 10^{-4}$	$\frac{3.25\ v^3}{v - 35}$

Table 1. Data at Low Flow Rates.

	Saccharin	Saccharin + 1% Cab-O-Sil	Carbowax 6000	Carbowax 6000 + 1% Cab-O-Sil	Cab-O-Sil
$Q_+ \frac{\mu C}{min} \times 10^8$	$823\ v$	$4.52\ v^2$	$3.05\ v^2$	$6.88\ v^2$	$18.8\ v^2$
$Q_- \frac{\mu C}{min} \times 10^8$	$5.20\ v^2$	$17.8\ v^2$	$123\ (v - 90)$	70×10^4	$2.53\ (v - 35) \times 10^4$
$W_+ \frac{\mu g}{min}$	1140	$10.0\ v$	$7.30\ v$	$31\ v$	183
$W_- \frac{\mu g}{min}$	$5.84\ v$	$25.2\ v$	120	$19\ v$	$5.07\ (1 - \frac{35}{v}) \times 10^3$
$W \frac{\mu g}{min}$	$175\ v^{1/2}$	$35.0\ v$	$7.30\ v$	$50\ v$	
$q_+ \frac{\mu C}{g} \times 10^3$	$7.22\ v$	$4.52\ v$	$4.18\ v$	$2.2\ v$	$1.05\ v^2$
$q_- \frac{\mu C}{g} \times 10^3$	$8.91\ v$	$7.06\ v$	$10.25\ (v - 90)$	$\frac{368}{v}$	$49.9\ v$
W_+ / W_-			$60.9\ v \times 10^{-3}$	1.63	
W_- / W_+	$5.10\ v \times 10^{-3}$	$5.10\ v \times 10^{-3}$			$27.7\ (1 - \frac{35}{v})$
$q_+ q_- (\frac{\mu C}{g})^2 \times 10^6$	$64.4\ v^2$	$31.9\ v^2$	$42.7\ v\ (v - 90)$	0.82×10^6	$52\ v^3$
$\frac{Q_+ Q_-}{W^2} (\frac{\mu C}{g})^2 \times 10^4$	$0.140\ v^2$	$656\ v^2 \times 10^{-4}$	$8.7\ (v - 90)$	1900	$190 \frac{v^4}{v - 35} \times 10^{-4}$

Table 2. Data at High Flow Rates.

	Saccharin	Saccharin + 1% Cab-O-Sil	Carbowax 6000	Carbowax 6000 + 1% Cab-O-Sil	Cab-O-Sil
AGGLOMERATION FACTORS AT v = 50 cc/min					
W_-/W_+ or W_+/W_-	4.0	4.0	0	1.5	1.2
$q_+q_-\left(\frac{\mu C}{g}\right)^2$	2.4	0.16	0	0.045	35
$P = \frac{Q_+Q_-}{W^2}\left(\frac{\mu C}{g}\right)^2$	0.56	0.035	0	1.6×10^{-9}	27
AGGLOMERATION FACTORS AT v = 500 cc/min					
W_-/W_+ or W_+/W_-	2.6	2.6	12*)	1.6	28
$q_+q_-\left(\frac{\mu C}{g}\right)^2$	16	8	9	0.8	6000
$P = \frac{Q_+Q_-}{W^2}\left(\frac{\mu C}{g}\right)^2$	3.5	1.6	0.35	0.19	250

*) Measured value

Table 3. Agglomeration Factors at V=50 cc/min and 500 cc/min.

below v = 90 cc/min and 12 times as many positive as negative particles at v = 500 cc/min. In both cases, the deagglomerant makes W_+ and W_- more equal, $W_+/W_- = 1.5$. As a result, the deagglomerant causes bonds between particles below v = 90 cc/min, but these bonds are comparatively weak, e.g., as compared to those in the case of saccharin + deagglomerant, and may not affect the flowability of the powder. At v = 500 cc/min, the bonds are stronger, but q_+q_- is still lower by a factor of 10 as compared to Carbowax 6000. The probability of collisions is reduced by a factor of 2 only. Thus, the deleterious effects of the deagglomerant are not important at low flow rates but are significant in the case of aerosols sprayed at high flow rates.

The agglomerations in the powder and in the aerosol in the aerosol generator can be studied by means of the aerosol density as given by W_+ and W_-. The conclusions drawn from these data are, of course, no more accurate than the data themselves. They will therefore be presented as tentative. They indicate a potential usefulness of the experimental technique for this type of investigation. It should be recalled that this use of the data was not anticipated during the actual experiments and that therefore no effort was made to control the aerosol density.

The weight and charge data show peculiarities at v = 200 cc/min for all materials except Carbowax 6000, and at v = 90 cc/min for Carbowax 6000 and at v = 35 cc/min for Cab-O-Sil At v = 90 cc/min, the linear flow rate is 300 cm/s and equal to that of the air stream at its entrance in the aerosol generator. At v = 35 cc/min, the linear flow rate is 120 cm/s and equal to that of the air stream at its exit from the aerosol generator. The particle sizes with these terminal velocities are approximately 600 and 240μ diameter, respectively. Although particles (or agglomerates) this large and much larger were present in the powders, it is not possible to relate these flow velocities with particle sizes without further experiments, particularly at different velocities of the air stream in the aerosol generator.

The linear velocity of the air stream through the aerosol generator was maintained at 3 cm/s. The maximum particle size that can be suspended in the aerosol at this velocity is approximately 25μ. Particles of this size have a considerable inertia. At low values of v they are not collected and the extent to which they are collected increases with v. Since the drag force is proportional to v^2 one may expect W to be proportional to v^2 at low flow rates. At high flow rates, W should be proportional to v at a constant aerosol density.

These considerations are reflected by the curves for W, W_+, and W_-. For saccharin (Figure 6), and saccharin + 1% Cab-O-Sil (Figure 6), W_+ is proportional to v^2 at low flow rates. Comparing the curves in Figure 19, we see that

$$W_+ = k_+ v^2 \tag{93}$$

$$W_- = k_- v \tag{94}$$

$$W = k_+ v^2 + k_- v \tag{95}$$

This indicates that the negative charge is carried by small particles without inertia, and that the positive charge is carried by large particles with considerable inertia. However, the curve of W_+ for saccharin + 1% Cab-O-Sil in Figure 6 shows no inertia effect at low flow rates.

The data for Carbowax 6000 + 1% Cab-O-Sil indicate that W, W_+, and W_- are all proportional to v^3 at low flow rates. In the case of Cab-O-Sil, W_+ is proportional to v at low flow rates, whereas W_- is zero below v = 35 cc/min.

Above v = 200 cc/min, W_+ for saccharin + 1% Cab-O-Sil appears to be independent of v. This means that the density d_+ is

$$d_+ = \frac{k}{v}, \quad v \geq 200 \frac{cc}{min} \tag{96}$$

Since 1/v is proportional to the time of residence t of the particles in the aerosol

$$d_+ = kt, \quad v \geq 200 \frac{cc}{min} \tag{97}$$

Accordingly, d_+ should be the density of agglomerates that fall out below v = 200 cc/min and that are all collected above v = 200 cc/min. Thus,

$$d_+ = kt_o, \quad v \leq 200 \frac{cc}{min} \tag{98}$$

when t_o is the residence time determined by fall-out.

Consequently, the positive charge should be carried by agglomerates formed in the aerosol. According to formulae (97) and (98), the rate of formation of these agglomerates is independent of d_+ .

The formula (93) together with the linear plot of Q_+ (Figure 2) gives

$$d_+ = \frac{274}{v}, \quad v \leq 200 \frac{cc}{min} \tag{99}$$

Thus, q_+ decays with increasing friction in the capillary tube. This is not improbable. A similar initial decay of the charge with increasing friction has been observed with glass beads. [2] Carbowax 6000 + 1% Cab-O-Sil shows a similar decay of q_- at high flow rates.

Since W_- is proportional to v, it is composed of particles with little inertia.

The same reasoning applied to Carbowax 6000 + 1% Cab-O-Sil suggests that all particles are large in the aerosol and that they agglomerate very rapidly in the aerosol. Indeed, the absence of a linear term in W indicates that all particles are large enough to show appreciable inertia. If we are to rely on the data, the particles are all of the maximum size, 25μ , and agglomerate at a rate such that

$$d = kv = \frac{k}{t}, \quad v \leq 200 \frac{cc}{min} \tag{100}$$

at low flow rates. This relation would apply to the case of rapid agglomeration according to the formula

$$-\frac{dd}{dt} = kd^2 \tag{101}$$

which gives

$$\frac{1}{d} - \frac{1}{d_o} \quad kt \tag{102}$$

and, when kt and d_o are large

$$d = \frac{1}{kt} \tag{103}$$

This seems to lead to a difficulty at high flow rates because the constant density at high flow rates requires that all particles and agglomerates are collected without inertia above v = 200 cc/min, whereas all agglomerates fall out below v = 200 cc/min. It appears, however, that if two 25μ particles collide while each is being sucked toward the capillary tube, they will continue to move toward the capillary tube.

The data for Carbowax 6000 are rather complex. However, it is clear that the inertia effect persists beyond v = 200 cc/min. The straight lines drawn for W and W_+ in Figures 9 and 7 are no more than very rough approximations. Above v = 300 cc/min, W and W_- decrease, probably as a result of extensive agglomeration in the powder after prolonged stirring. It is noteworthy that the aerosol density is small as compared to that for Carbowax 6000 + 1% Cab-O-Sil.

Comparing the plots of W for saccharin + 1% Cab-O-Sil and Carbowax 6000 + 1% Cab-O-Sil at high flow rates, we see that both aerosols have small enough particles not to show an inertia effect, and that the density of the latter aerosol is larger than that of the former aerosol. But the data at low flow rates indicate larger particles in the latter than in the former aerosol. It should then follow that there are smaller particles in the former powder but less of them, i.e., the saccharin + 1% Cab-O-Sil powder is more agglomerated than is the Carbowax 6000 + 1% Cab O-Sil powder. As a consequence, the former powder should have a range of particle size from small unagglomerated particles to very large agglomerates, whereas the latter powder should have a more uniform size of agglomerates of about 25μ with none of the small unagglomerated particles and little of the very large agglomerates. This seems to be in accord with observations on the effects of the deagglomerant upon the flowabilities of the two materials.

An important conclusion, as yet tentative, is that the effect of the deagglomerant is to form agglomerates of the order of 25μ and of

a fairly uniform size. These agglomerates flow more readily than the powder particles because the forces between the agglomerates are smaller than those between the original particles, which prevents them from agglomerating, and because the flow at a uniform particle size should be easier than at a large variation in particle size. However, the forces that break up agglomerates in flow are not present in the aerosol, and a reduction of the agglomerate size in a flowing powder by no means indicates a limitation to the agglomerate size in the aerosol.

The decay of q_- for Carbowax 6000 + 1% Cab-O-Sil for $v \geq 200$ cc/min and that of q_+ in the range 200 to 300 cc/min indicate a transfer of charge from the negative particles to the positive particles. Carbowax 6000 alone being predominantely positive and Cab-O-Sil alone being predominantely negative, the two combine such that the negative Cab-O-Sil particles form a coat on the positive Carbowax 6000 particles.[5] The Cab-O-Sil particles would thus tend to bind Carbowax 6000 particles together. If now two such agglomerates, one covered with Cab-O-Sil, the other bare, collide and stick together, their subsequent separation would break the bonds between the Cab-O-Sil and either the former or the latter agglomerate. In the former case, both agglomerates lose charge while remaining negative and positive, respectively. Thus q_+ and q_-, and Q_+ and Q_- may change while W_+ and W_- are unchanged. Thus, positive and negative particles may collide and agglomerate in the aerosol and then be broken up by friction and impact in the capillary tube on their way to the charge analyzer.

The charge distributions found with these materials differ very drastically from some of those found previously with other materials[6]. Thus, for MgO and NH_4Cl, $W_+ = W_-$ at all flow rates. For polyvinyl chloride, both W_+ and W_- were proportional to v and $W_-/W_+ = 2.5$ at all flow rates. For Buerker's powder W_+/W_- was 4 at low flow rates and increased with the flow rate at high flow rates.

It appears that this difference may be a result of the technique for producing the aerosol. The aerosol generator shown in Figure 1 was used for polyvinyl chloride and Buerker's powder. MgO was produced by burning a strip of Mg metal and NH_4Cl was produced by mixing NH_3 and HCl vapors. In both cases the aerosol was produced in a comparatively large glass cylinder. The MgO and NH_4Cl aerosols were close to monodisperse, whereas the aerosols produced in the aerosol generator cannot be monodisperse because of

agglomeration into particles of widely varying sizes. W_+/W_- would be expected to vary with the particle size distribution.

The effect of the particle size distribution upon the particle charge distribution was not studied in this investigation. It appears to be an important factor in the control of particle charge.

It should be pointed out that the charge per gram is greater for small particles than for large particles. This was found in the preceding investigation[6], and it is also shown clearly in the large charge values for Cab-O-Sil in Tables 1 and 2.

Reference was made in Section 2 to an observation, as yet tentative, that the flowing material may not coat the tube wall at very low humidities. This tentative observation should be investigated. If confirmed, it means that the charge distribution may be controlled by a suitable choice of nozzle material, e.g., by inserting a sleeve of a suitable material in the nozzle. It would also mean, of course, that the data obtained at 10% RH do not apply at lower humidities because if there is no coat there is no charge. However, these data should still apply to electrification under conditions where a coated tube wall is not involved, e.g., in milling and slow flow.

7. CONCLUSION

This investigation was undertaken in order to learn more about the electrification of airborne particles in the flow through a tube, and in order to determine the charge and the charge distribution on the particular materials used. The results show that these measurements are useful in the evaluation of deagglomerants. They also indicate means for the control of the charge and charge distribution of sprayed aerosols.

The data obtained yield information on the tendency to agglomeration in powders and aerosols. They show that the charge distribution may depend very much upon the flow rate, and that it may be possible to produce unipolar aerosols by using a high enough flow rate in spraying. The effect of a deagglomerant may vary very much with the flow rate and may be very different with different materials. Thus, Cab-O-Sil is effective with saccharin at low flow rates but has no effect at high flow rates.

In order to take full advantage of the information yielded by these measurements, one should correlate it with direct observations of agglomerates and agglomeration and with the particle size distribution. It is hoped that future investigations may be extended in these directions.

Meanwhile, the data obtained yield information on the electrification of the materials investigated. Of particular interest is that the charge distributions differ so much with the materials studied, namely, from almost equal amounts of positively and negatively charged particles to almost complete predominance of one polarity or the other.

To the problem of aerosol stability it is important that the charge increases with the flow rate, and that it becomes increasingly unipolar as the flow rate increases. This has a profound bearing upon the control of aerosol charge and aerosol stability.

In the application of measurements of this type to the spraying of aerosols, the coating of the tube wall by the aerosol material is a decisive factor. This factor should be investigated, particularly at low humidities. There is evidence to the effect that the composition of the gas used in spraying affects the charge and charge distribution of the aerosol.[6] This may be an important factor in the control of aerosol charges, and it should be investigated from this point of view.

Important conclusions, although as yet tentative, can be drawn on the effects of deagglomerants. A deagglomerant may cause free flow by forming large agglomerates, which are limited in size and smaller than those formed in the pure material. This is ruinous to presized aerosol particles. A deagglomerant may cause a change in charge distribution so that there are equal abundances of positive and negative particles, whereas the pure material may be close to unipolar. This promotes agglomeration in the aerosol.

It should be noted that there are no or very weak forces only on aerosol particles, whereas the forces on powder particles in flow are quite large. The fact that a powder flows freely is no indication that agglomeration in its aerosol would not occur.

It appears that the effects mentioned are inherent with deagglomerants. These effects should be carefully studied before a deagglomerant is added to a presized aerosol material.

4% RH for silica sand[3] and at 7% RH for plexiglass[4]. It is difficult to handle fine powders at high humidities, and, in practice, dry powders for aerosol production will be held at some technically achievable low humidity. In the work of Nash et al[5] in this field, the relative humidity was held at 2%. It appears that a still lower humidity, say, 0.5% RH, would be preferable and also attainable.

It was shown in other preceding investigations[8, 9] that collisions between aerosol particles are determined by electrostatic forces. Oppositely charged particles collide as a result of electrostatic attraction, particles of equal polarity are prevented from colliding by electrostatic repulsion. This holds at all humidities of the air.

The data presented in Section 2 were obtained at a comparatively high humidity, 10%. They apply directly to collisions in aerosols sprayed at 10% RH. They also apply directly to agglomeration in powders, for which electrostatic adhesion predominates at 10% RH. They apply indirectly to agglomeration in powders at lower humidities on the assumption that the charge distribution is essentially the same at the lower humidities, whereas the charge level may be higher at the lower humidities. The data will be discussed on this basis in this section and in Section 6

Agglomeration may be discussed in terms of forces of adhesion within the agglomerates and the number of particles engaged in agglomerates. At low humidities, the former quantity is determined essentially be the magnitude of the charge; the latter quantity is determined essentially by the charge distribution. In the cases under consideration there were no neutral particles. Hence, agglomeration occurs with oppositely charged particles only.

The number of particles engaged in agglomerates, ν, may be expressed in terms of W_+/W_-. When this quantity is zero or infinite, i.e., for unipolar charge, there are no agglomerates, and ν is therefore zero for these two values of W_+/W_-. When $W_+/W_- = 1$, all the particles may be engaged in agglomerates, and ν has therefore a maximum at $W_+/W_- = 1$.

As the size of an agglomerate increases, the external forces acting upon it also increase. It is conceivable that the agglomerate grows by addition of particles of successively smaller charges. The size of the agglomerates should thus be determined by the force of adhesion.

REFERENCES

1. H. Göhlich, VDI-Forschungsheft No. 467, Suppl. to Forsch. Geb. Ingenieurw. B24(1958).

2. T. G. Owe Berg and T. A. Gaukler, Aerojet-General Corp., Ordnance Div., Downey, Calif., Special Report No. 0395-04(05)SP, March 1963.

3. T. G. Owe Berg, M. J. Hunkins and M. J. Stansbury, Aerojet-General Corp., Ordnance Div., Downey, Calif., Special Report No. 0395-04(04)SP, March 1963.

4. T. G. Owe Berg and M. J. Stansbury, Aerojet-General Corp., Ordnance Div., Downey, Calif., Special Report No. 0395-05(12)SP, Oct. 1963.

5. J. H. Nash et al, Final Report, Contract No. DA-18-108-405-CML-829, 1963.

6. T. G. Owe Berg, G. C. Fernish and W. J. Flood, Aerojet-General Corp., Ordnance Div., Downey, Calif., Special Report No. 0395-04(08)SP, May 1963.

7. T. G. Owe Berg, Aerojet-General Corp., Ordnance Div., Downey, Calif., Special Report 0395-03(10)SP, Dec. 1961.

8. T. G. Owe Berg and N. Brunetz, Arch. Environm. Health 5(1962)16.

9. T. G. Owe Berg, Aerojet-General Corp., Ordnance Div., Downey, Calif., Special Report No. 0780-01(02)SP, Sept. 1963.